



The Precambrian of Transangaria, Yenisei Ridge (Siberia): Neoproterozoic microcontinent, Grenville-age orogen, or reworked margin of the Siberian craton?



Alexander B. Kuzmichev^{a,*}, Eugene V. Sklyarov^{b,c}

^a Geological Institute of Russian Academy of Sciences, 7 Pyzhevsky Pereulok, Moscow 119017, Russia

^b Far Eastern Federal University, 8 Sukhanov Street, Vladivostok 690950, Russia

^c Institute of the Earth's Crust, Siberian Branch of the Russian Academy of Sciences, 128 Lermontov Street, Irkutsk 664033, Russia

ARTICLE INFO

Article history:

Received 17 April 2015

Received in revised form 8 October 2015

Accepted 22 October 2015

Available online 23 October 2015

Keywords:

Yenisei Ridge

Precambrian of Siberia

Siberian craton

Central Asian Orogenic Belt

U–Pb geochronology

ABSTRACT

The Yenisei Ridge was traditionally perceived as an uplifted segment of the western Siberian craton affected by Neoproterozoic collision events. However, the suggestions for Archaean or Palaeoproterozoic ('Siberian') basement in Transangaria have not been confirmed by reliable geochronological data. A new view regards most of the Ridge, namely, its Transangarian segment, to be an exotic Neoproterozoic terrane that collided with Siberia in the late Neoproterozoic. This paper presents new U–Pb SHRIMP zircon ages demonstrating that Archaean rocks (2611 ± 12 Ma) actually exist in this territory. We also provide a review of published U–Pb zircon ages for igneous and metamorphic rocks of Transangaria together with our new age data. This geochronological dataset clarifies the geology of the Yenisei Ridge and leads to new conclusions, as follows. (1) It is likely that Transangaria was originally underlain by an Archaean–Palaeoproterozoic basement, similar to that of the Siberian craton. (2) Geochronological data do not confirm the idea of widespread "Greenvillian age" granitoides in Transangaria. (3) The Neoproterozoic evolution of the Yenisei Ridge segment of the Siberian craton margin includes the following events. (i) Collision of an unidentified terrane with the western margin (in recent coordinates) of the Siberian craton during 900–855 Ma. The colliding terrane is no longer present in the current structure. (ii) Dextral shearing during 830–800 Ma may have been caused by counter-clockwise rotation of the Siberian craton. (iii) Extensional conditions prevailed during 800–700 Ma. The Isakovka oceanic basin formed at this time interval. (iv) Thrusting of the Isakovka island arc and accretionary prism onto the Siberian margin occurred during the late Neoproterozoic (650–630 Ma) and caused high-pressure metamorphism.

© 2015 Elsevier Ltd. All rights reserved.

1. Introduction

The Yenisei Ridge represents the largest region of Precambrian rocks exposed along the western margin of the Siberian Platform (Fig. 1). The Ridge has been a traditional gold mining region since the 19th century. In the 1950s and 1960s, the territory was covered by medium-scale (1:200000) State Geological Mapping. Later, 1:50000 scale surveys were conducted, and a new generation of geological maps is currently being compiled. Nonetheless, many geological issues of this area remain unresolved, including uncertainties concerning the general tectonic features and the Precambrian evolution. One of the reasons for many geological uncer-

tainties is the fact that the entire territory of the Yenisei Ridge is densely forested, and outcrops are mainly found along river banks.

The Angara River divides the Yenisei Ridge into two unequal parts, which are the Angara-Kan block in the south and the Transangaria block in the north (Fig. 2). The Angara-Kan block is a fragment of the crystalline basement of the marginal part of the Siberian craton. It is composed of granulite, gneiss, charnockite and other early Precambrian rocks. Metamorphic rocks of the Angara-Kan block were described in detail by Kusnetsov (1941). This researcher distinguished two units, the Kan and Yenisei Groups. Transangaria is an area where late Precambrian rocks predominate. The cumulative thickness of the Meso- and Neoproterozoic metasedimentary sequences exceeds 15 km. For many years, these sequences were compared with the stratotype Riphean sedimentary series of the Ural Mountains. Not long ago, geologists had no doubt that Transangaria is underlain by an ancient

* Corresponding author.

E-mail addresses: nsi.kuzmich@yandex.ru (A.B. Kuzmichev), skl@crust.irk.ru (E.V. Sklyarov).

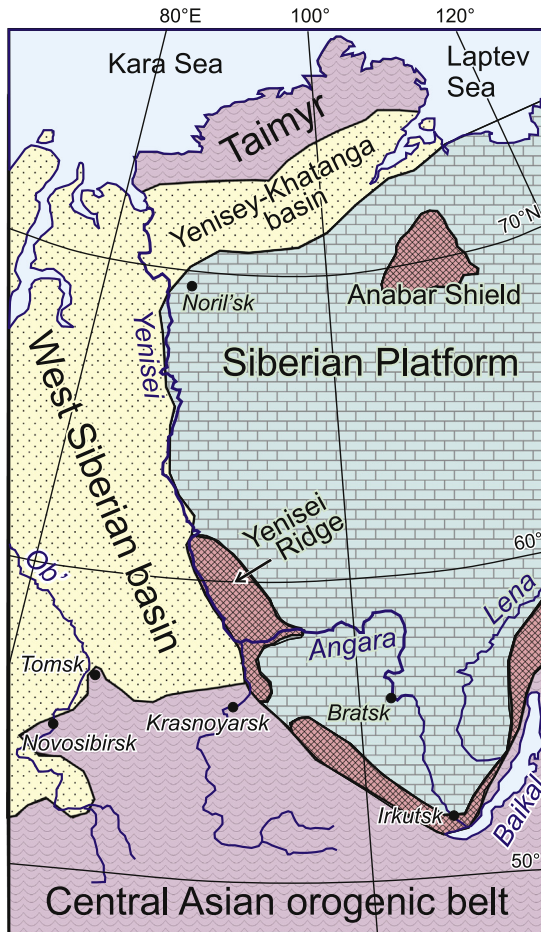


Fig. 1. General location of the Yenisei Ridge.

crystalline basement of the Siberian craton that is the same as in the southern part of the Ridge. The presence of old rocks appeared to be partly confirmed by isotopic ages (e.g., Volobuev et al., 1976, and references therein); however, none of these old age data have ever been reproduced using modern techniques of isotope geochronology. The oldest rock reliably dated in Transangaria is a granite-gneiss of the Nemtikha metamorphic unit (1360–1380 Ma; Popov et al., 2010). Therefore, the presence of Palaeoproterozoic and/or Archaean rocks has been questioned (Vernikovskiy et al., 2003).

The tectonic interpretation of the Yenisei Ridge structure depends on the basement age. According to Vernikovskiy et al. (2003, 2007), most of Transangaria belongs to the so-called Central Angara terrane (Fig. 2), which is an exotic block unrelated to the Siberian craton. During most of the Precambrian, this terrane evolved as a part of another palaeocontinent or microcontinent that drifted in the Palaeo-Asian ocean. It was suggested that Transangaria collided with the Siberian craton in the late Neoproterozoic (760–720 Ma ago; Vernikovskiy et al., 2003, 2007). Accepting this interpretation means that the geological events revealed in Transangaria for the time interval earlier than 760 Ma are related to the evolution of one of Precambrian terranes scattered within the Central Asian Orogenic Belt (CAOB), rather than the Siberian margin.

The above views are not shared by all researchers. Geologists who mapped Transangaria for several decades, have reinterpreted the earlier data and recognised two metamorphic units, namely Nemtikha and Malogarevka that presumably contain Archaean rocks (Kachevskiy et al., 1994). These units were correlated with the Kan and Yenisei Groups of the Angara-Kan block and can thus be considered as belonging to the basement of the Siberian craton.

Kachevskiy et al. (1998) published a geological map of the Yenisei Ridge (scale 1:500000) that shows the extent of the above units in a large portion of Transangaria, including the region of our investigation (Figs. 3 and 4). However, here are no geochronological data to confirm the ancient age of these units. On the other hand, the Archaean age of the Kan and Yenisei Groups of the Angara-Kan block is also not confirmed by isotopic dating. Granulite-facies metamorphism was dated as Palaeoproterozoic, whereas an Archaean age has only been obtained for rare relict zircon cores (Bibikova et al., 1993; Turkina et al., 2012; Urmantseva et al., 2012).

A new interpretation suggesting the presence of Grenville-age granitoids and metamorphic rocks in Transangaria has been proposed, based on chemical U–Pb ages for monazite (Likhanov et al., 2012, 2014, 2015 and references therein). Currently, all data published by the Likhanov team are presented in terms of either accretion or the break-up of Rodinia.

In view of these contradictory concepts of the Yenisei Ridge geology, the available geological data cannot be easily interpreted in terms of either the Precambrian evolution of the Siberian cratonic margins, the relationship between Siberia and Rodinia or the Neoproterozoic evolution of the CAOB. This paper attempts to clarify the situation.

The first author studied the Yenisei Ridge in the early 1980s when the traditional ideas of its geology were widely accepted (Kuzmichev, 1987). Later the territory was reinvestigated, including outcrops of metamorphic rocks that were classified as Archaean by Kachevskiy et al. (1994, 1998). Information on two such sites is given below. These are the Vyatka region in the south and the Yenisei bank near the Proklyataya River in the north (Fig. 4). In addition, we review recently published zircon ages for Transangaria to correlate the recognised events with the geology

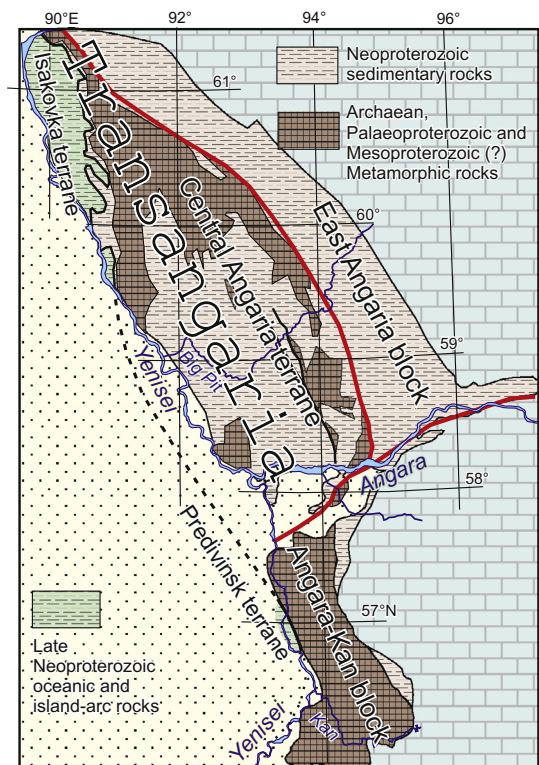


Fig. 2. Main geological subdivisions of the Yenisei Ridge. The red line is a contour of the Central Angara terrane of Vernikovskiy et al. (2003, 2007), who suggested it to have collided with Siberia at 760–720 Ma. (For interpretation of the references to colour in this figure legend, the reader is referred to the web version of this article.)

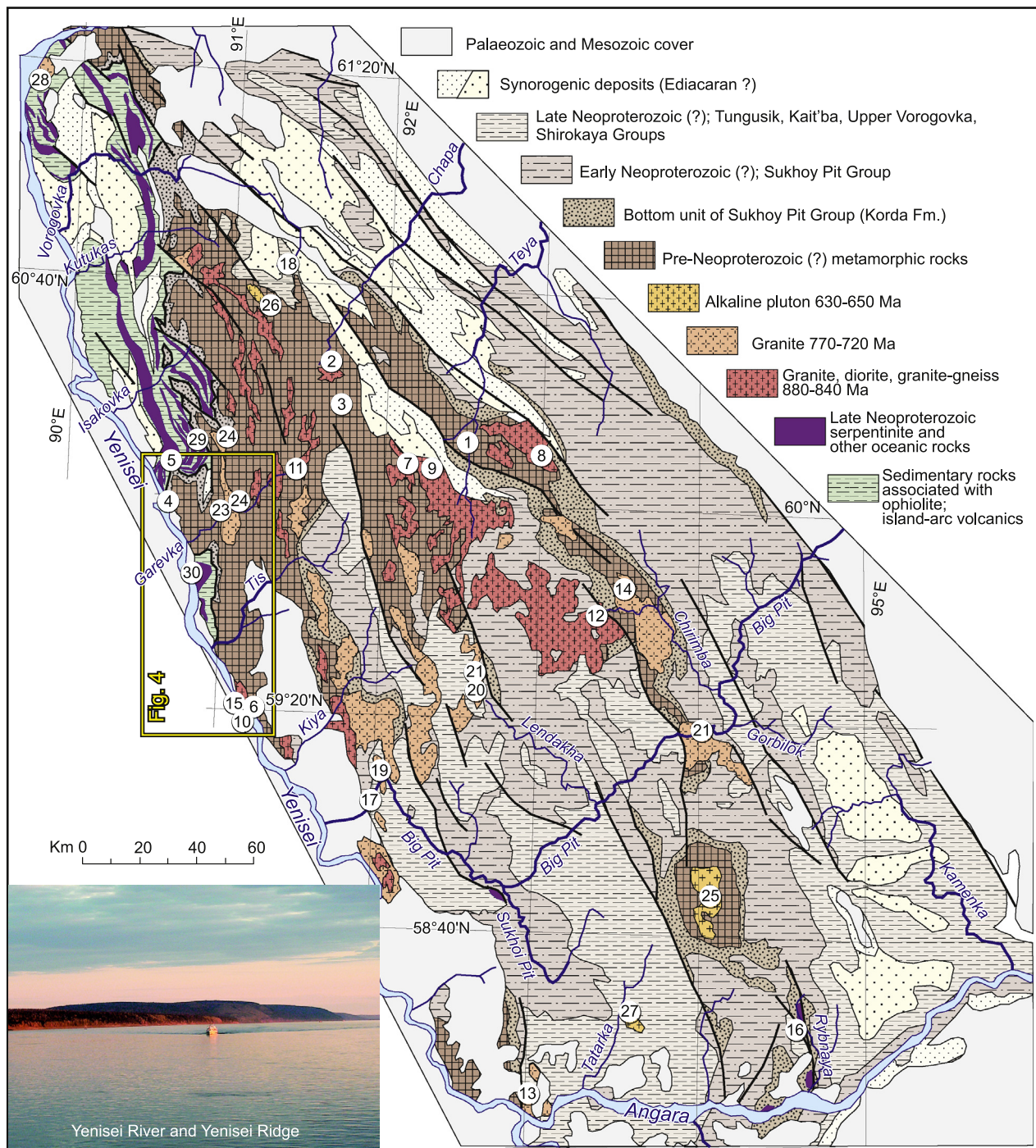


Fig. 3. Simplified geological map of Transangaria, adapted from Kachevsky et al. (1998) and State Geological Maps. The encircled numbers show the locations of dated rocks used in the review of available U–Pb zircon ages (see Section 5). Numbers correspond to those in Figs. 16–18.

in the rest of the Yenisei Ridge. This analysis provides data to reveal succession of Neoproterozoic events in the Transangarian segment of western margin of the Siberian craton.

2. The Vyatka Site: 'Taraka-type' migmatites and augen-gneisses

2.1. Geological overview

The exposures of granitoids and metamorphic rocks studied in the Vyatka region are shown in Fig. 5A. The metamorphic rocks are represented by biotite-, garnet-biotite, and two-mica schists,

rare amphibolites and quartzites, which are typical of all Mesoproterozoic and some Neoproterozoic units in Transangaria. They are partly migmatized or were converted to granite-gneiss, blastomylonite or augen-gneiss and display no sign of possible Archaean high-grade metamorphism, assumed by Kachevsky et al. (1998, see Fig. 4). Locally they are cut by pegmatite and granite dykes. Excellent outcrops dissected by the Yenisei River are located on the south-eastern shore of Ostrovok island and on the bank of the Yenisei River (Fig. 5A). These outcrops were studied in detail (Fig. 5B and C).

The migmatite is well exposed at the northeastern shore of Ostrovok Island (Fig. 5B). The exposure shows biotite and

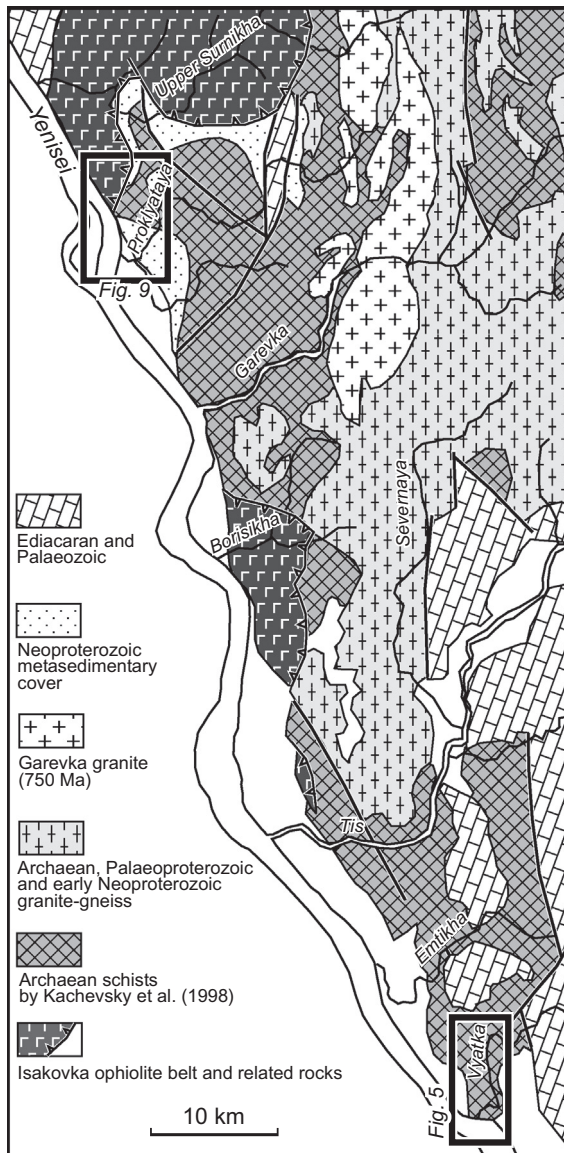


Fig. 4. General view of the study area (simplified after Kachevsky et al., 1998).

garnet–biotite schists invaded by leucosome of trondhjemitic composition with bluish quartz (Fig. 6A and B). According to Nozhkin (personal communication), the migmatite is the oldest observable metamorphic high-temperature phase in the area similar to that in the surroundings of Palaeoproterozoic Taraka granite pluton in the Angara-Kan block (Nozhkin et al., 2009). A leucosome lens was sampled for dating (sample 11/2).

The above migmatite is cut by pegmatite veins. The latter are composed of quartz and blocky red-coloured¹ K-feldspar with occasional flakes of muscovite. Zircons were extracted from the vein shown in Fig. 6C (sample 11/3). Southwards, at Point 12 (see Fig. 5B), a gradual transition from migmatite to augen-gneiss is exposed. The augen gneisses contain orthoclase porphyroblasts, typically intergrown with quartz and locally grading into small lenses of leucosome (Fig. 6D and E). Such porphyroblastic gneisses make up most of the exposed part of Ostrovok Island. They formed during dextral shearing. Two types of their protoliths are distinguishable. Most augen-gneisses formed after metapelites, and K-feldspar crystals grew during deformation. Some varieties formed after

granite protoliths. Both types display transitions to blastomylonite and mylonite. Red microcline granite with slight foliation was found at the south-western shoreline of Ostrovok Island (point 18, Fig. 5B). The granite is cut by K-feldspar pegmatite, tourmaline pegmatite and quartz veins.

The augen-gneisses are common in western Transangaria adjacent to the Yenisei River. They mark a shear zone or a set of zones that are several tens to several hundred metres wide. Pegmatite veins and dykes are closely related to augen-gneisses, and their orientation, as a rule, is consistent with dextral shearing. Pegmatites were not affected by high-temperature deformation. They intruded during the final phase of shearing. Dating of pegmatite emplacement will determine the time at which shearing ended.

The rocks exposed at the Yenisei River bank at a location called Vyatka Stones (Fig. 5C) are similar to those on Ostrovok Island. In the western part of this outcrop, blastoporphyratic K-feldspar gneissic granite is dominant. Westwards, this grades into blastomylonite (Fig. 6F and G). Near Point 37 (Fig. 5C) the granite-gneiss contains dykes (up to 30 cm) of light-yellow leucogranite (Fig. 6H) that was sampled for dating (sample 37/1-05). To the east, at point 39, biotite-, garnet–biotite, two-mica, and staurolite-schist crop out, and near the outlet of the Vyatka River, migmatites similar to those of Ostrovok Island are exposed (Fig. 5C).

2.2. SHRIMP zircon geochronology

Isotope analyses were conducted at the Centre of Isotopic Studies of the All-Russian Geological Institute (VSEGEI), St. Petersburg, using the SHRIMP II ion microprobe. Sample preparation and isotope measurements were carried out by standard techniques described by Williams (1998). The primary oxygen ion flow ($I \sim 3.5$ nA) was focused onto a $25 \times 35 \mu\text{m}$ spot. The measurement results were referenced to the zircon standard 91500 (age = 1062.4 Ma, U/Pb = 0.17917, Wiedenbeck et al., 1995) and averaged over four scanning cycles. Data reduction, age calculation, and concordia plot construction were made using the SQUID and ISOPLOT programs (Ludwig, 2001, 2003). Three zircon samples were analysed, namely 11/2-05 – a migmatite from the Ostrovok Island, 11/3-05 – a pegmatite vein intruding the migmatite, and 37/1-05 – a dyke of aplite-like granite that cuts blastoporphyratic granitoids near the mouth of the Vyatka River. The $^{206}\text{Pb}/^{238}\text{U}$ ratio used for age estimation of individual concordant analyses, which is more precise than $^{207}\text{Pb}/^{238}\text{U}$ for ages younger than 1 Ga (e.g. Gehrels, 2012). The age of zircon crystallization for clustered concordant analyses was calculated as ‘concordia age’, which is more accurate than weighted mean (Ludwig, 2003). Some samples revealed complex age distribution, and number of performed analyses was not sufficient for confident age estimation. Reported data for such samples should be regarded as provisional.

The migmatite sample 11/2-05 provided brownish to colourless long-prismatic zircon crystals, which showed distinct relict cores and metamorphic rims in cathodoluminescence (CL) images (Fig. 7A and B). Four analyses of rims show a high uranium (1800–2500 ppm) and low thorium (Th/U = 0.01–0.02) content (Table 1), suggesting crystallisation from a fluid phase. Two rims show concordant age of 830 Ma, two others are younger up to ~ 800 Ma (Table 1, Fig. 8A). It is most likely that younger ages indicate lost of radiogenic Pb due to subsequent thermal event (see sample 11/3-05 below).

Three analyses were performed on the zircon cores. Two analyses involved dark high-uranium (3000–5000 ppm) cores that appear homogeneous in CL images and do not display any apparent zoning (Fig. 7B). Such cores are dominant among zircons in the sample; they are metamict in some crystals due to the high concentration of uranium. The cores contain little thorium, which usually referred to metamorphic origin. Some cores display magmatic

¹ For interpretation of colour in Figs. 6, 17 and 18, the reader is referred to the web version of this article.

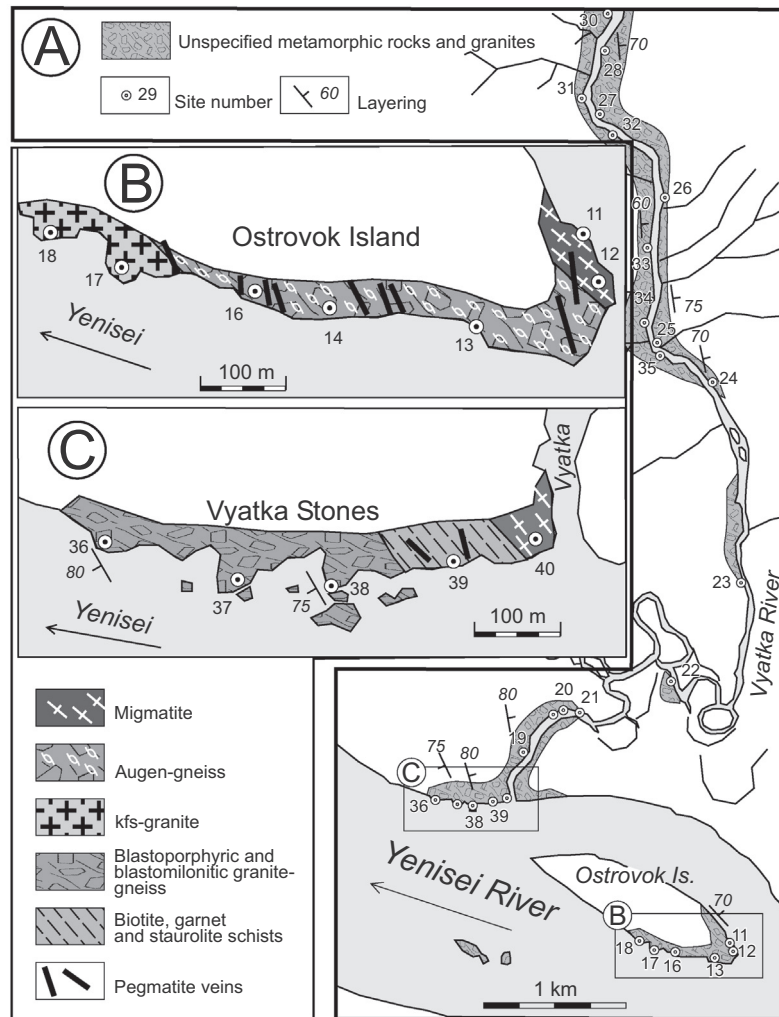


Fig. 5. Bedrock exposures in the Vyatka region. (A) General layout. (B and C) Detailed location of exposures on Ostrovok Island and at the Vyatka Stones.

oscillation zoning and a magmatic Th/U ratio (#5.1 in Table 1). All three cores provided the same age and form a concordant cluster with an age of 900 ± 3 Ma (Fig. 8A), which we consider as the age of zircon crystallization during anatexis under fluid influence. Spot 8.1 (Table 1) appears to show a thin overgrowth rim that is oriented in the polished plane of the sample (Fig. 7A, spot 8.1). This analysis indicates an intermediate age between the rims and cores, because some portions of both rim and core were sampled.

The pegmatite sample 11/3-05 contained large brownish, fractured zircons. In CL images, they appear dark due to a high uranium contents (2400–5500 ppm, see Table 1). Their zoning is not clear, and some grains are metamict (Fig. 7C). Their Th/U ratio is 0.01–0.06. The zircons yielded variable ages, despite their similarity in CL images. The two oldest grains have $^{206}\text{Pb}/^{238}\text{U}$ ages of about 830 Ma, which is the same as the age of metamorphic rims of the sample 11/2-05. Six other grains constitute a concordant cluster with an age of ~ 800 Ma (797 ± 2 Ma, Fig. 8B). The two youngest grains have lost some of radiogenic lead soon after pegmatite emplacement. This sample confirms the age of the zircon rims in sample 11/2-05 (830–800 Ma); however, the majority of zircons crystallized ~ 800 Ma ago. Judging from the two samples, we suggest that the process of augen-gneiss formation and the intrusion of the accompanying pegmatites occurred in the time interval at 830–800 Ma.

The aplitic dyke sample 37/1-05 (Fig. 6H) contains transparent zircons and some crystals are cloudy in the centre. The crystal edges are smoothed, probably resulting from dissolution. In CL images (Fig. 7D), they appear dark, and oscillatory zoning is poorly visible. Indistinct metamict cores are present in some crystals. All eight analysed crystals have high uranium contents (from 2000 to 4500 ppm) along with high thorium contents and have a magmatic Th/U ratio (Table 1). The four oldest grains make up a cluster with an age of 770 ± 2 Ma, and we assume that this correspond to the time of granite crystallisation (Fig. 8C). Other analyses distributed along concordia toward 710 Ma. They partially lost radiogenic lead, possibly during emplacement of younger granites.

The last assumption is supported by data for a subalkaline leucocratic granite from a small rocky island in the Yenisei River in front of the Vyatka mouth, dated by Likhonov et al. (2013). Six zircons (from 12 analysed) yielded a concordant cluster at 748 ± 7 Ma (2σ). Three other grains partially lost radiogenic lead and their analytical points may be connected with the previous six by a discordia that yields an upper concordia intercept age of 747 ± 14 Ma. The remaining three older crystals constitute a concordant cluster at 770 ± 11 Ma (2σ), which coincides with the above age of our sample 37/1. The data of Likhonov et al. (2013) confirm the magmatic event at 770 Ma and also confirm the above assumption that the event was not the last one in the Vyatka region.



Fig. 6. Typical rocks in the Vyatka region. (A–E) Ostrovok Island (Fig. 5B); (F–H) Vyatka Stones (Fig. 5C). (A) Migmatite on the south-eastern shore of Ostrovok Island (point 11; hammer for scale). (B) Lens-shaped leucosome vein with bluish quartz (width of photo 20 cm). A similar vein was dated (sample 11/2). (C) Quartz–feldspar pegmatite vein cutting migmatite between points 11 and 12. The host migmatite is visible in the top left corner (photo is 25 cm wide). Sample 11/3 was taken from this vein. (D) Lineation in augen gneiss visible on two planes near point 14. (E) Sigmoid leucosome in blastomylonite and the S-C cleavage suggesting dextral shearing (area between points 14 and 16). (F) Blastoporphyritic granite-gneiss near point 36. (G) Blastomylonite at point 38. (H) Aplitic dyke (dated sample 37/1) in host granite-gneiss at point 37. Marker length is 17 cm.

Thus, we did not find the Archaean rocks in the Vyatka region. Nevertheless, the above results are important for a better understanding of the Neoproterozoic tectonics in Yenisei Ridge. The processes that took place in the time interval 900–750 Ma are discussed in Sections 5 and 6.

3. The Proklyataya River-Ostyatski brook region

3.1. General remarks

While planning our study of this area, we expected to find two principal geological boundaries, i.e., the boundary of an Archaean basement and the Meso-(?) to Neoproterozoic cover (i), and the thrust sole of the Isakovka ophiolite belt (ii) (see Fig. 4). However in field, distinctions between the above main suites along assumed contacts were not evident. In the schematic map of the area (Fig. 9A), the dashed (i.e., inferred) lines show the contours of the main exposed units. Their boundaries are shown by continuous curved contours; however, there is no doubt that locally they are

displaced by faults. Most faults are either syn-metamorphic or pre-metamorphic and are represented by zones of foliation, boudinage and blastomylonitisation abundant through territory. Most observations were made along the Proklyataya River (Fig. 9B) and on the bank of the Yenisei River (Fig. 9C).

3.2. Proklyataya River

Rocks that could be interpreted as a metasedimentary cover that overlies an old basement (see Fig. 4) were only found in the area near the outlet of the Proklyataya River (Fig. 9B) where metamorphic rocks include quartzite horizons. Most of the riverside outcrops show quartz–biotite, two-mica, and garnet schist, amphibolite, garnet amphibolite, and andalusite schist. Augen-gneisses (Fig. 10A) and pegmatite veins similar to those of the Vyatka Site are also widespread (Fig. 9B).

In the northernmost part of the traversed segment along the river, conceivably more ancient rocks are exposed, which are represented by migmatite and gneiss. An upper contact is visible

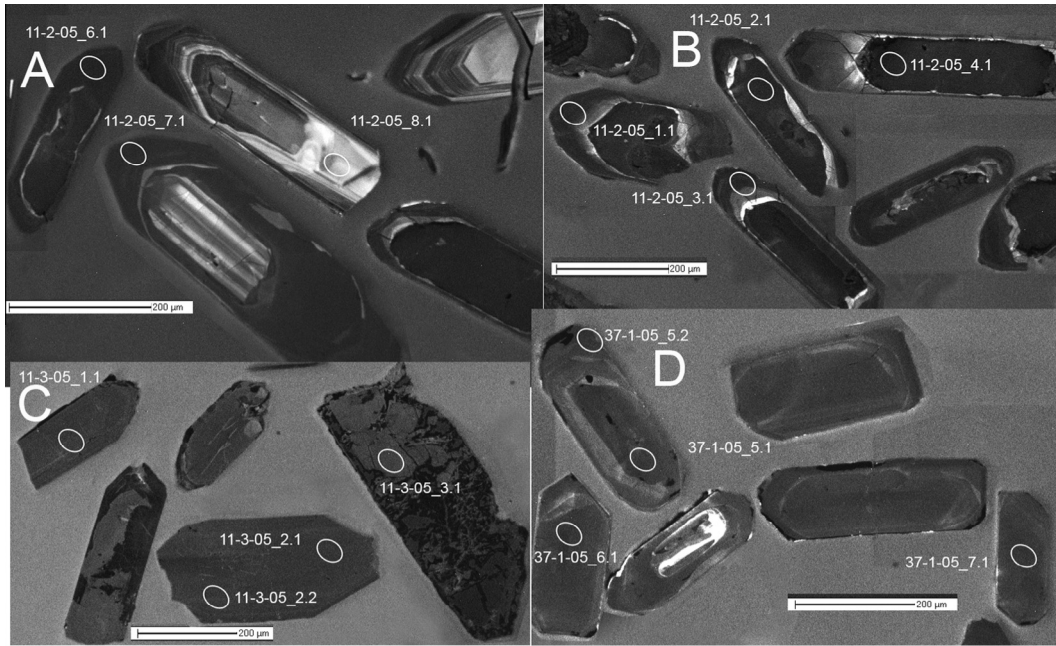


Fig. 7. Representative CL zircon images from rocks of the Vyatka region. Ovals indicate analysed spots. Spot numbers correspond to those in Table 1. Bar length is 200 μm. (A and B) Migmatite sample 11/2-05. Zircon cores do not show igneous zoning. Rims are lighter at the inside and darker at the outside. Cores and rims differ in age, and both are predominantly represented by metamorphic zircon with low Th/U ratios. A crystal can be seen at the bottom of photo A, whose core displays oscillatory zoning. A similar core was analysed (spot 5.1, Table 1) and revealed the same age as the dark cores. (C) Pegmatite sample 11/3-05. High-uranium, partly metamict crystals with indistinct zoning. (D) Aplitic granite sample 37/1-05. Zoning is not distinct but, contrary to the other samples, the crystals have a magmatic Th/U ratio. Cores and rims have similar ages.

Table 1
U and Pb isotopic data for zircons of Vyatka area.

Spot No. (r – rim, c – core)	% ²⁰⁶ Pb _c	ppm U	ppm Th	²³² Th/ ²³⁸ U	ppm ²⁰⁶ Pb [*]	(1) Age (Ma) by ²⁰⁶ Pb/ ²³⁸ U	(1) Age (Ma) by ²⁰⁷ Pb/ ²³⁵ U	%D	(1) ²⁰⁷ Pb [*] / ²⁰⁶ Pb [*]	±, %	(1) ²⁰⁷ Pb [*] / ²³⁵ U	±, %	(1) ²⁰⁶ Pb [*] / ²³⁸ U	±, %	Error corr.
<i>Migmatite 11/2-05</i>															
11-2-05_6.1 r	0.01	2544	44	0.02	287	796.3 ±2.5	787 ±14	-1	0.06539	0.67	1.1854	0.75	0.13148	0.33	0.445
11-2-05_3.1 r	0.02	2315	18	0.01	266	810.2 ±2.2	796 ±14	-2	0.06567	0.67	1.2125	0.73	0.13391	0.29	0.394
11-2-05_1.1 r	0.00	1790	14	0.01	211	827.7 ±3.0	845 ±16	2	0.06723	0.75	1.2700	0.84	0.13700	0.38	0.452
11-2-05_7.1 r	0.01	2521	23	0.01	297	827.9 ±2.6	830 ±14	0	0.06674	0.66	1.2612	0.74	0.13704	0.33	0.451
11-2-05_8.1 r	0.74	199	46	0.24	25	871.9 ±8.8	797 ±100	-9	0.06570	4.80	1.3120	4.9	0.14480	1.1	0.222
11-2-05_4.1 c	0.00	5132	89	0.02	659	898.6 ±2.0	878 ±37	-2	0.06830	1.80	1.4090	1.8	0.14958	0.24	0.132
11-2-05_2.1 c	0.04	3285	104	0.03	423	899.8 ±2.5	911 ±12	1	0.06940	0.58	1.4333	0.65	0.14979	0.30	0.457
11-2-05_5.1 c	3.96	623	368	0.61	84	902 ±5.8	972 ±110	8	0.07150	5.20	1.4810	5.2	0.15020	0.69	0.132
<i>Pegmatite 11/3-05</i>															
11-3-05_3.1	0.00	2396	24	0.01	265	781.4 ±2.5	778 ±14	0	0.06511	0.67	1.1569	0.75	0.12886	0.33	0.445
11-3-05_8.1	0.03	3060	125	0.04	342	788.9 ±2.2	781 ±14	-1	0.06520	0.68	1.1703	0.74	0.13019	0.30	0.406
11-3-05_5.1	0.01	3702	181	0.05	416	792.3 ±2.3	804 ±14	1	0.06591	0.65	1.1885	0.72	0.13078	0.31	0.433
11-3-05_2.1	-	3960	196	0.05	446	793.6 ±1.7	815 ±10	3	0.06626	0.50	1.1968	0.55	0.13100	0.23	0.425
11-3-05_1.1	0.01	4167	227	0.06	470	795 ±2.0	810 ±10	2	0.06612	0.50	1.1966	0.56	0.13126	0.27	0.469
11-3-05_2.2	-	4178	210	0.05	473	797.8 ±2.0	795 ±11	0	0.06564	0.50	1.1923	0.57	0.13174	0.27	0.476
11-3-05_5.2	-	3662	181	0.05	415	798.6 ±2.2	798 ±12	0	0.06572	0.57	1.1951	0.64	0.13188	0.29	0.453
11-3-05_4.1	0.02	4649	227	0.05	528	800.3 ±2.0	816 ±10	2	0.06631	0.50	1.2084	0.57	0.13217	0.26	0.465
11-3-05_6.1	0.01	5508	213	0.04	649	827.9 ±1.7	798 ±19	-4	0.06572	0.91	1.2420	0.93	0.13705	0.22	0.238
11-3-05_7.1	-	4024	164	0.04	476	832 ±2.0	805 ±12	-3	0.06596	0.58	1.2528	0.63	0.13776	0.25	0.398
<i>Granite 37/1-05</i>															
37-1-05_4.1 c	0.27	2352	972	0.43	236	710.8 ±4.0	729 ±36	3	0.06360	1.70	1.022	1.8	0.11657	0.60	0.338
37-1-05_2.1 c	0.28	2445	1005	0.42	254	732.5 ±3.6	726 ±31	-1	0.06353	1.50	1.054	1.5	0.12035	0.52	0.337
37-1-05_1.1 r	0.08	4602	398	0.09	487	747.6 ±2.3	747 ±21	0	0.06416	1.00	1.088	1.1	0.12297	0.33	0.309
37-1-05_3.1	0.22	2962	1524	0.53	314	747.9 ±3.7	720 ±34	-4	0.0634	1.60	1.074	1.7	0.12302	0.53	0.308
37-1-05_5.2 r	0.06	1974	438	0.23	214	765.4 ±2.5	786 ±17	3	0.06536	0.80	1.1361	0.87	0.12606	0.35	0.403
37-1-05_5.1 c	0.03	2590	623	0.25	282	769.1 ±1.9	757 ±13	-2	0.06447	0.64	1.1263	0.69	0.12671	0.27	0.387
37-1-05_6.1 c	0.05	3199	1604	0.52	349	770.2 ±2.2	770 ±14	0	0.06487	0.67	1.1351	0.73	0.12691	0.30	0.405
37-1-05_7.1	0.02	3374	1046	0.32	370	773.8 ±1.8	765 ±12	-1	0.06472	0.58	1.1382	0.63	0.12755	0.25	0.401

Errors are 1σ; Pb_c and Pb* indicate the common and radiogenic portions, respectively. (1) Common Pb corrected using measured ²⁰⁴Pb.

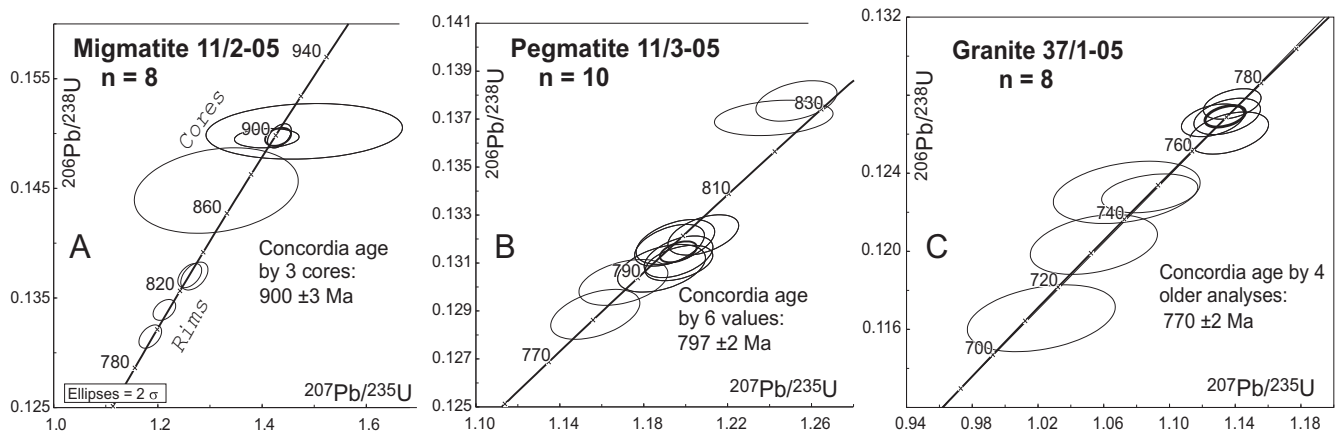


Fig. 8. Concordia diagrams for zircons analyses from the Vyatka region. Error ellipses are 2σ . (A) Migmatite sample 11/2-05. (B) Pegmatite sample 11/3-05. (C) Granite sample 37/1-05.

near point 119 (Fig. 9B), where gently dipping trondhjemitic gneiss is overthrust from the west by augen-gneiss and other K-feldspar-bearing rocks. The least altered garnet–two-mica schists and migmatites are exposed at point 122 (Fig. 9B) where they are cut by quartz–tourmaline veins. Overall, it appears that the Proklyataya rocks do not differ much from those of the Vyatka region.

3.3. Outcrops along the bank of the Yenisei River

On the well-exposed bank of the Yenisei River the Isakovka allochthon is deformed and metamorphosed together with underlying units, and the exact thrust boundary cannot be easily identified. Most rocks of the Isakovka ophiolite belt lost their characteristic features, and serpentinite remains the only rock that can be confidently identified as belonging to the Isakovka unit. The southernmost serpentinite body enters the area of Fig. 9C. The Isakovka rocks once more appear on the Yenisei bank farther south (Fig. 9C). In this area, the Isakovka unit includes amphibolite, as well as mica-ankerite schist, which sometimes contain fuchsite flakes. Less metamorphosed fuchsite and ankerite micaceous sandstone and schist are typical of the lower part of the Isakovka unit along the Upper Surnikha River (Fig. 4). Amphibolites included in the Isakovka unit in Fig. 9C are foliated and boudinaged (Fig. 10B and C), and look similar to those of the genuine Isakovka belt north of the map boundary. They are also similar to ophiolitic flaser gabbro described from the Borisikha area (Kuzmichev et al., 2008).

At this site, a Neoproterozoic sedimentary cover of the old continental block can be reliably identified as it contains dolomite of the Letnyaya Formation (Fig. 10D). Carbonate rocks occasionally crop out between points 138 and 144 (Fig. 9C) and were also observed south of the Ostyatski brook in 1980. In addition, metaconglomerate containing carbonate pebbles is present in the southern outcrop. The cover sequence also contains quartzite that is usually interbedded with quartz–biotite and garnet–biotite schist. The lower unit is composed of metapelite and augen-gneiss that are similar to the above rocks of the Vyatka Site and along the Proklyataya River.

The inferred boundaries of the above geological units are shown as continuous lines in Fig. 9, which are curved to vergent folds. It is also possible that the structure is different and represents a series of tectonic slices thrust from the west–northwest. The oldest rocks (see below) exposed at the site are found near the outlet of the Ostyatski brook (Fig. 9C).

3.4. The oldest rocks near the outlet of the Ostyatski brook

At this site (Fig. 11), bedrocks are exposed at the sloped strand of the Yenisei River mostly as isolated patches partially covered with pebbles (Fig. 10E). The main outcrops are numbered in Fig. 11 and rock compositions are given in the legend. The oldest rocks are predominantly represented by garnet amphibolite and crop out at sites 3–5. Outcrops 2 and 3a represent a wide transition zone from common biotite schist and augen-gneiss in the east to garnet amphibolite in the west. A transition zone on the north-western side of the domain of old rocks (see #6 in Fig. 11) is dominated by quartz–biotite (\pm plagioclase), amphibole–biotite schist and trondhjemitic. Carbonate is present in almost all rock types. The central part of outcrop #6 is composed of actinolite schist with boudins of gabbro-amphibolite and fine-grained melanocratic amphibolite. In the westernmost part of the outcrop, foliated carbonate-rich micaceous rocks are found.

At outcrops 3, 4 and 5, the rocks are apparently different from those of the surrounding areas. Three closely related rock types were only found at these outcrops, namely melanocratic garnet amphibolite, tonalite, and carbonatite.

Amphibolite appears as a black or greenish-black medium-grained rock containing variable amounts of garnet (Fig. 10F). In the north-western part of outcrop 3, garnet grains are surrounded by reaction rims of plagioclase. These rocks differ from the garnet amphibolite of the Isakovka belt, which are exposed in the same region, e.g., at the top left corner of Fig. 9A. The Isakovka garnet amphibolites are composed of actinolite, albite, epidote, and chlorite, and have a pale greenish-grey appearance. The Ostyatski brook garnet amphibolites are composed of dark bluish-green hornblende crowded with needles of ore mineral in the central parts of grains. The rocks also contain plagioclase, carbonate, garnet, biotite, chlorite, titanite, apatite, and zircon.

Tonalite (metatonalite) veins (up to 50 cm wide) in the garnet amphibolites (Fig. 10G) are composed of fine-grained quartz–plagioclase aggregates with biotite and occasional garnet. Rare relics of large plagioclase crystals (up to 5 mm) are also found. Quartz and plagioclase are xenomorphic and show cataclasis and dynamic recrystallisation at grain boundaries. Biotite (up to 15%) forms flakes, which may be replaced by chlorite. The rock also contains secondary (?) carbonate in varying amounts. A high LOI (loss on ignition) in chemical analysis was caused by the presence of carbonate and chlorite (Table 2). Plagioclase is zoned and the central parts are speckled with epidote. At some locations the rock

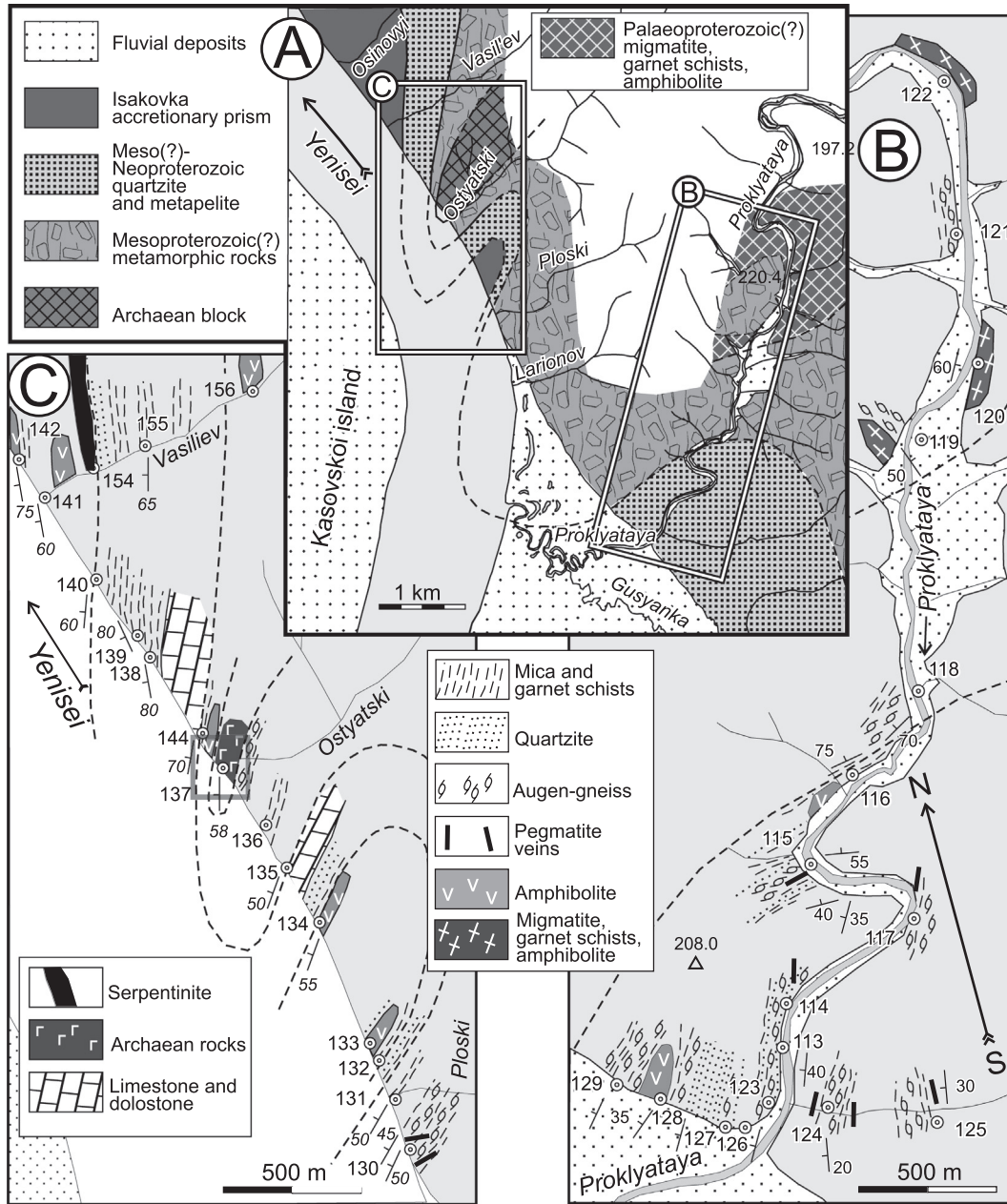


Fig. 9. Simplified geological sketch maps for the Proklyataya River and nearby Yenisei River bank. Dotted lines indicate inferred geological boundaries. These boundaries are tentatively shown as continuous lines depicting coherent folds, although the structure can also be interpreted as a series of thrust slices. (A) General layout. (B) Proklyataya River. (C) Yenisei shore between Ploski and Vasiliev brooks. Rectangle corresponds to Fig. 11.

contains partly dissolved relicts of hornblende. The initial contours of amphibole crystals are still outlined in places by tiny epidote and ore mineral segregations.

Carbonatite veins are composed of calcite and dolomite, in which siderite may reach 25%. Usually, the surfaces of such veins are rusted (Fig. 10H). In addition to carbonate, these rocks contain biotite, occasional greenish light mica, chlorite, actinolite and hornblende, quartz and accessory ilmenite, titanite, zircon and, rarely, rutile. If the veins are located in garnet amphibolite, they contain relict garnet and hornblende grains. Calcite is the youngest mineral phase that 'cements' clusters of fine-grained dolomite (Fig. 12A). Dolomite grains have a distinct zonal structure where the central part is composed of pure dolomite surrounded by low-iron dolomite (up to 10% siderite) zone, whereas the rim consists of iron-rich dolomite (up to 25% siderite). Calcite occurs in the interstices between dolomite grains.

We label these rocks as carbonatite due to their undoubtedly intrusive nature. Their mineralogical and geochemical features indicate that they are most likely crustal carbonatites, melted out of sedimentary carbonate rocks under high H₂O partial pressure. A model of carbonate melting under crustal conditions was proposed by Lentz (1999). Examples of injected carbonate and silicate-carbonate rocks, which were indisputably emplaced as melts are known throughout the world, including the West Baikal region, Russia (Liu et al., 2006; Wan et al., 2008; Sklyarov et al., 2013).

We only have two chemical analyses for metaigneous rocks, one for the dominating garnet amphibolite and one for a dated tonalite (Table 2). Amphibolite 137/5 corresponds to high-titanium, high-iron picritic basalt that is typical for an intraplate setting. The concentrations of incompatible elements, including rare earth elements (REE), are high, and the chondrite-normalised REE

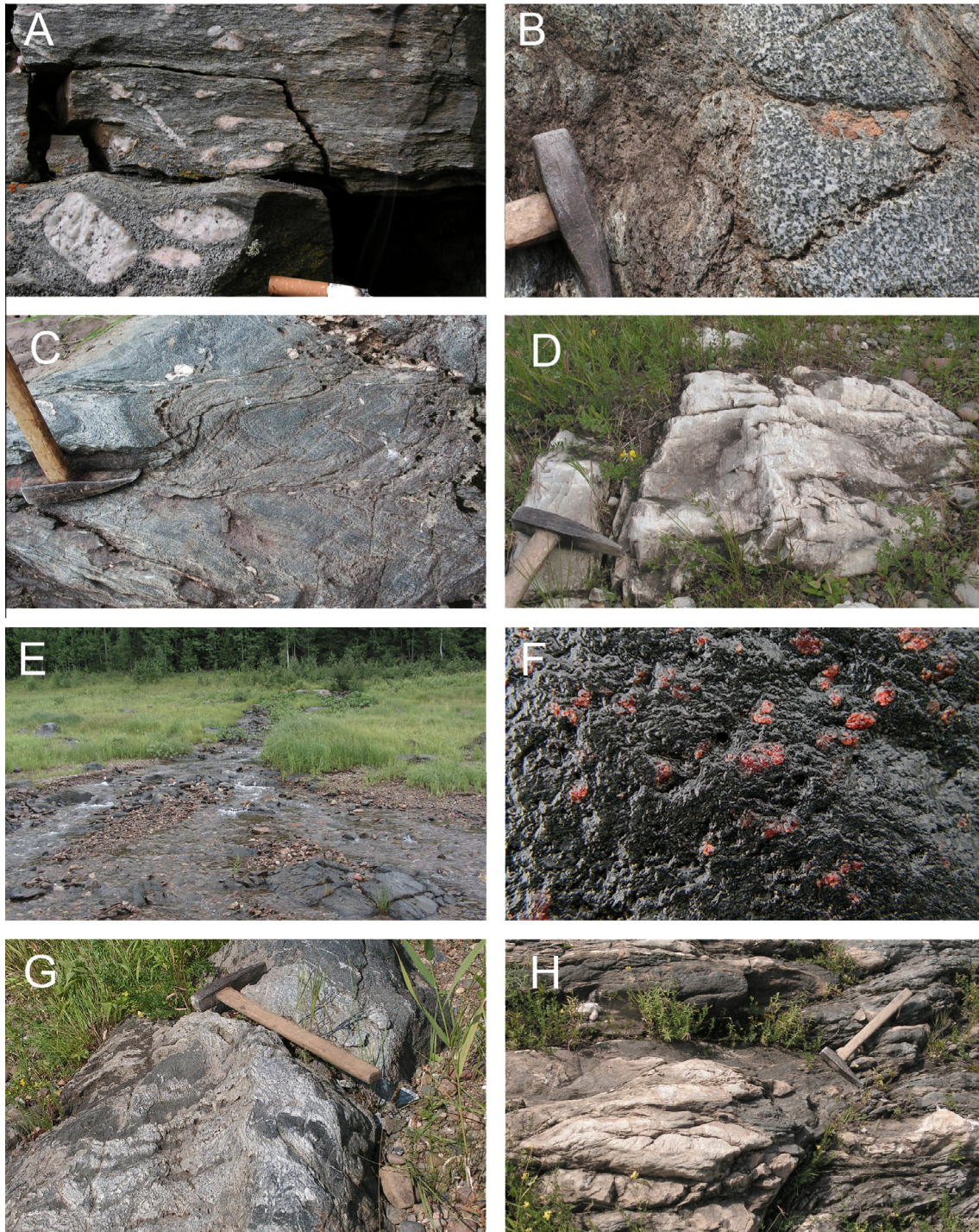


Fig. 10. Typical rocks exposed along the Proklyataya River and Yenisei bank, which are referred to in the text. (A) Augen gneiss – blastomylonite at point 127 (Fig. 9B). Sigmoidal-shaped porphyroblasts and clockwise rotation of idiomorphic orthoclase crystal in the lower left corner indicate dextral shearing during porphyroblast growth. Such kinematics are consistent with orientation of the leucosome veinlet (on the left), that fills the extensional crack. Field of view is 20 cm. (B and C) Amphibolite at point 134 (Fig. 9C) that are assumed to belong to the Isakovka ophiolite belt. (B) Metagabbro boudin. (C) Deformed banded amphibolite (flaser-gabbro). (D) Dolostone of Letnyaya Fm. on the beach near point 144 (Fig. 9C). (E) General view at the Ostyatski brook outlet where Archaean amphibolites are exposed. (F) Archaean garnet amphibolite (field of view is 9 cm). (G) Archaean tonalitic veins near mouth of Ostyatski brook. (H) Deformed carbonatite veins in outcrop 4 (see Fig. 11).

pattern is relatively flat (Fig. 13A and B). The rock contains a high amount of Ta and Nb and shows low Th/Nb and La/Nb ratios. The latter is indicative of an intraplate environment, such as an oceanic plateau or a volcanic island (Condie, 1999).

Tonalite sample 137/7 has lower concentrations of REE that are more strongly differentiated (Fig. 13B). This may indicate a genetic relationship between the two rock types. Most REE, especially the

heavy REE, as well as yttrium, may be retained in garnet: specifically these components are depleted in the tonalite. This is supported by a multi-element variation diagram (Fig. 13A) where tonalite and amphibolite display complementary positive and negative anomalies of Ti, Ta and Nb. The above elements are concentrated in refractory mineral phases and may remain in the restite, if tonalite is melted out of a mafic rock. If so, it is likely that

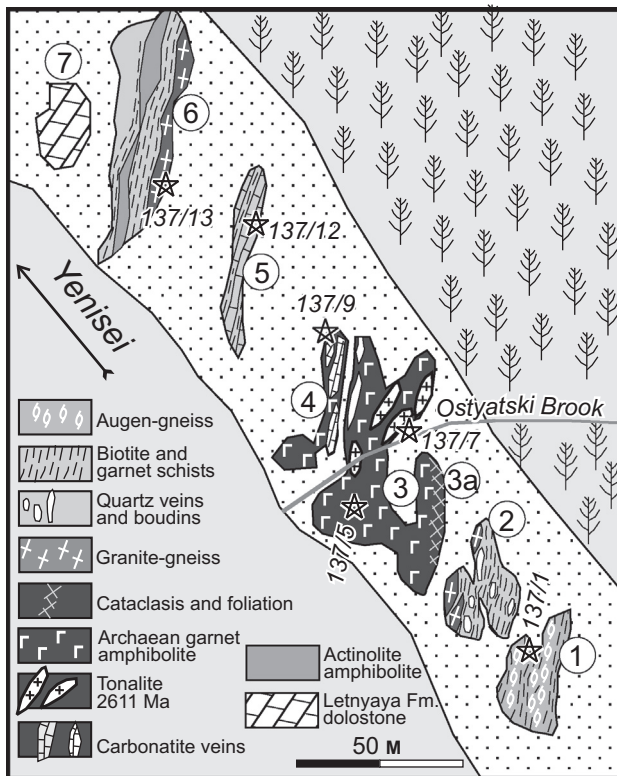


Fig. 11. Sketch of metamorphic rocks exposed on the bank of the Yenisei River near the mouth of the Ostyatski brook, where Archaean rocks were found. The outcrops are numbered, and their descriptions are given in Section 3.4. Stars with numbers indicate locations of samples mentioned in the text.

picritic rock sample 137/5 had a different mineral composition during tonalite melt extraction. Hornblende mainly concentrates the medium REE and, on melting would produce a specific REE pattern of the melt, which is different from that of 137/7.

3.5. Dating of the Ostyatski tonalite

Zircons from tonalite sample 137/7 are slightly rounded because of dissolution and subsequent metamorphic overgrowth. They are yellowish brown to colourless with elongation ratios from 1:2 to 1:4. In CL images (Fig. 14) the zircons display a combination of sector and oscillatory zoning, which resemble CL pattern of granulite zircons (e.g. Vavra et al., 1996). Almost all crystals are similar in habitus and zoning, and can be considered to reflect a uniform population. Overgrowth rims are clearly visible on most grains (Fig. 14). Typically, these rims are thin but wide enough on several grains for SHRIMP analysis.

In total, 13 isotopic analyses were performed on nine crystals (cores and rims). Nine core results are well grouped on concordia at 2600 Ma, and four rims define a cluster near 830 Ma (Fig. 15A). The cores are characterised by high Th/U ratios (up to 3.5, Table 3), which correspond to high Th/U value of parental melt (9.5, Table 2) and require PT environment where concurrent mineral phase such as monazite is unstable (e.g. Belousova et al., 2002). The error ellipses for analyses 3.1 and 6.1 lie above concordia due to excess Pb (Fig. 15B), and are excluded from further consideration. Seven other analyses with old ages form a compact concordant cluster slightly elongated in the direction of Pb loss. The calculation of a discordia line anchored at zero results in an upper intercept age at 2611 ± 12 Ma, MSWD = 0.89 (Fig. 15B). If we assume that Pb loss occurred at the time of rim formation, all but two analytical points (3.1 and 6.1) can be fitted to a discordia

Table 2

Chemical composition of two Archaean metaigneous rocks: garnet amphibolite 137/5-05 and tonalite 137/7-05. Oxides concentrations are given in weight%, minor elements in ppm.

	SiO ₂	TiO ₂	Al ₂ O ₃	Fe ₂ O ₃	MnO	MgO	CaO	Na ₂ O	K ₂ O	P ₂ O ₅	LOI	Total																
137/5-05	44.94	2.97	13.9	18.08	0.26	7.1	9.51	0.8	0.73	0.27	1.48	100.03																
137/7-05	61.59	0.56	13.71	4.58	0.15	2.79	5.99	4.34	0.61	0.2	5.48	99.98																
	Sc	V	Cr	Ni	Rb	Sr	Y	Zr	Nb	Ba	La	Ce	Pr	Nd	Sm	Eu	Gd	Tb	Tm	Yb	Lu	Hf	Ta	Th	U			
137/5-05	44.5	413	65.4	81.4	18.2	90.8	48.8	195	41.4	168	15.6	44.3	6.51	28	7.9	2.42	8.38	1.46	8.65	1.7	4.83	0.67	4.7	0.65	5.09	2.57	2.37	3.53
137/7-05	5.9	65.9	31	22.7	18.9	204	11.7	134	13.6	140	35.8	62.2	6.39	21.5	3.85	1.34	3.56	0.45	2.13	0.44	1.04	0.13	0.69	0.13	3.32	0.8	9.66	1.02

Major oxides analysed by X-ray diffraction method at the UIGGM, Novosibirsk, minor components by ICP-MS in All-Russian Geological Institute, St. Petersburg.

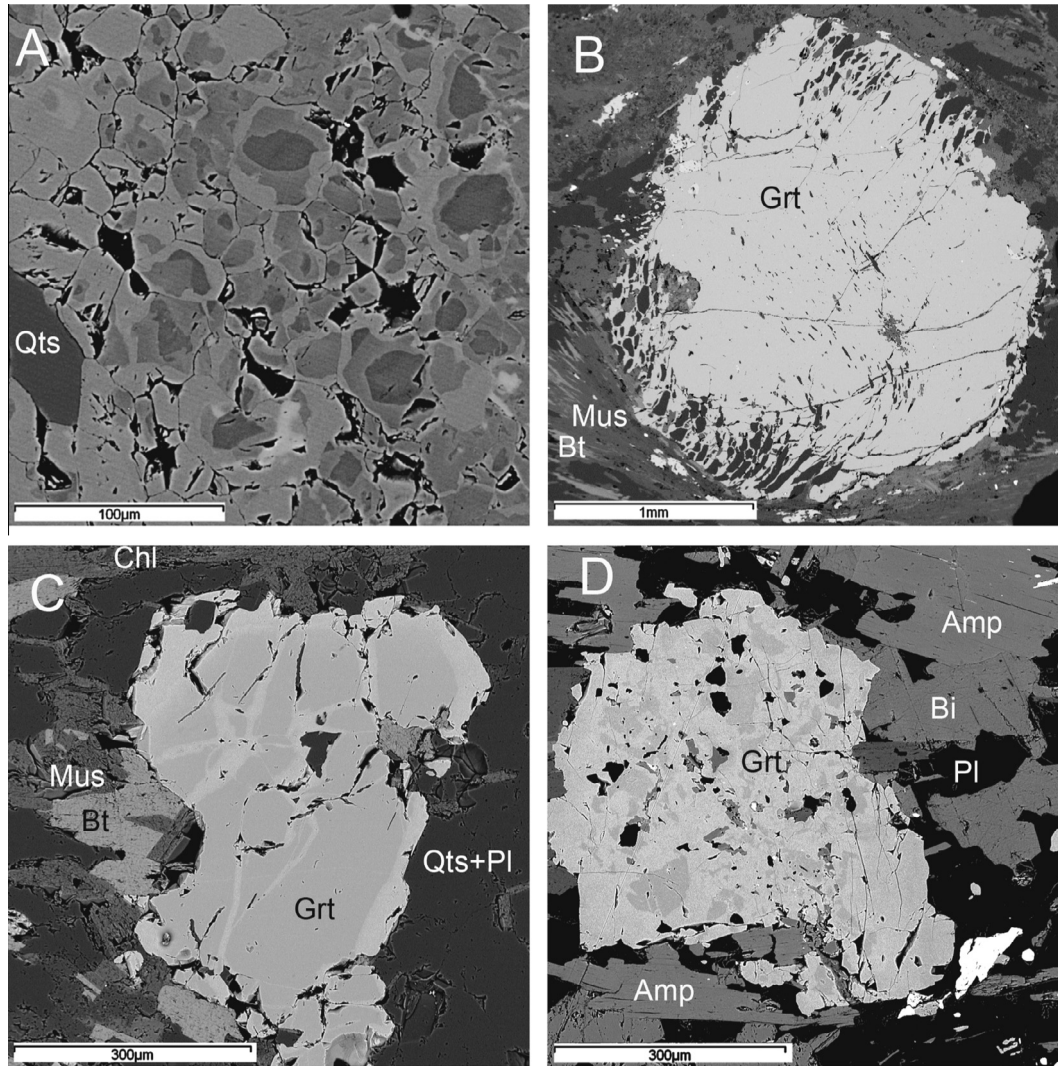


Fig. 12. Back scattered images of dolomite carbonatite (A), garnet in schists (B, C) and garnet in amphibolite (D) from the Yenisey bank between the Ploski and Ostyatski brooks. Mineral abbreviations after [Whitney and Evans \(2010\)](#): Amp – amphibole; Bt – biotite; Chl – chlorite; Grt – garnet; Pl – plagioclase; Qtz – quartz. (A) Structure of dolomite carbonatite sample 137/9 ([Fig. 11](#)). Centre – pure or low-ferrous dolomite (dark); transition zones – ferrous dolomite (FeO = 4–5 weight%); margins – higher ferrous dolomite (FeO = 8 weight%). Calcite (lightest) is found in the interstices. (B) Sigmoidal morphology of quartz inclusions in garnet suggesting syn-deformational growth (sample 131/3); (C and D) replacement of early high-Ca garnet by late garnet along fractures and at margins. (C) In garnet–two mica schist sample 137/1. (D) In garnet–biotite amphibolite sample 132/12.

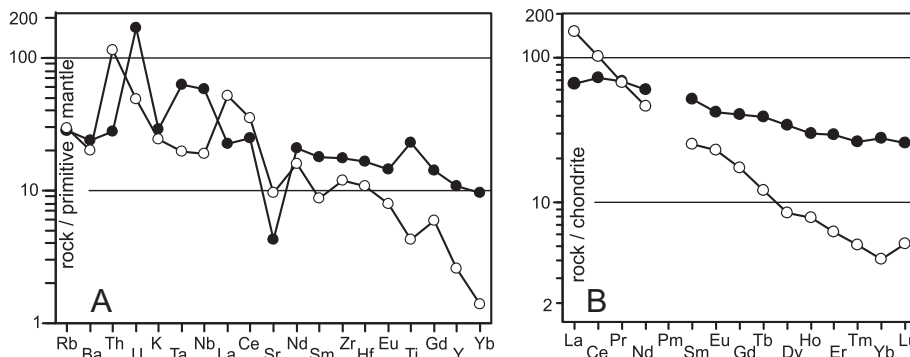


Fig. 13. Normalised multielement variation (A) and REE (B) diagrams. Normalising values from [Sun and McDonough \(1989\)](#). Dark circles denote amphibolite sample 137/5; light circles denote tonalite sample 137/7.

with an upper concordia intercept age of 2614 ± 15 Ma and a lower intercept at 817 ± 32 Ma and an MSWD of 0.38 ([Fig. 15A](#)).

The rims are composed of “metamorphic” zircon with an extremely low Th/U ratio ([Table 3](#)), which implies fluid involvement in

zircon crystallization. Four rim analyses lie on concordia ([Fig. 15C](#)), and their $^{206}\text{Pb}/^{238}\text{U}$ ages vary from 850 ± 14 to 813 ± 14 Ma ([Table 3](#)). Considering the range of errors they are statistically equal and their age can be calculated as a concordant cluster of

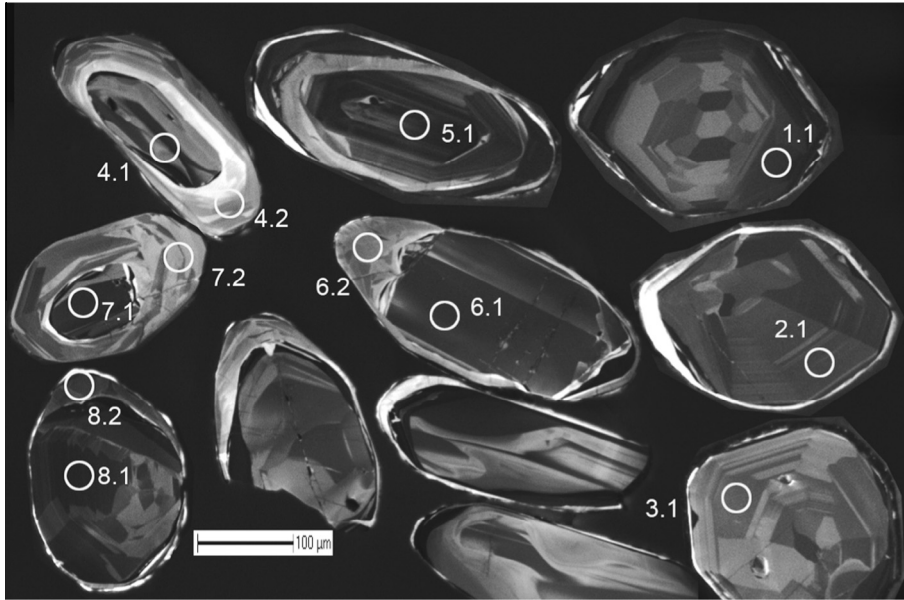


Fig. 14. CL images of zircons from tonalite sample 137/7-05. Archaean (~2.6 Ga) cores and Neoproterozoic (~830 Ma) metamorphic rims are clearly visible. Spot numbers correspond to those in Table 3. Scale bar is 100 μm.

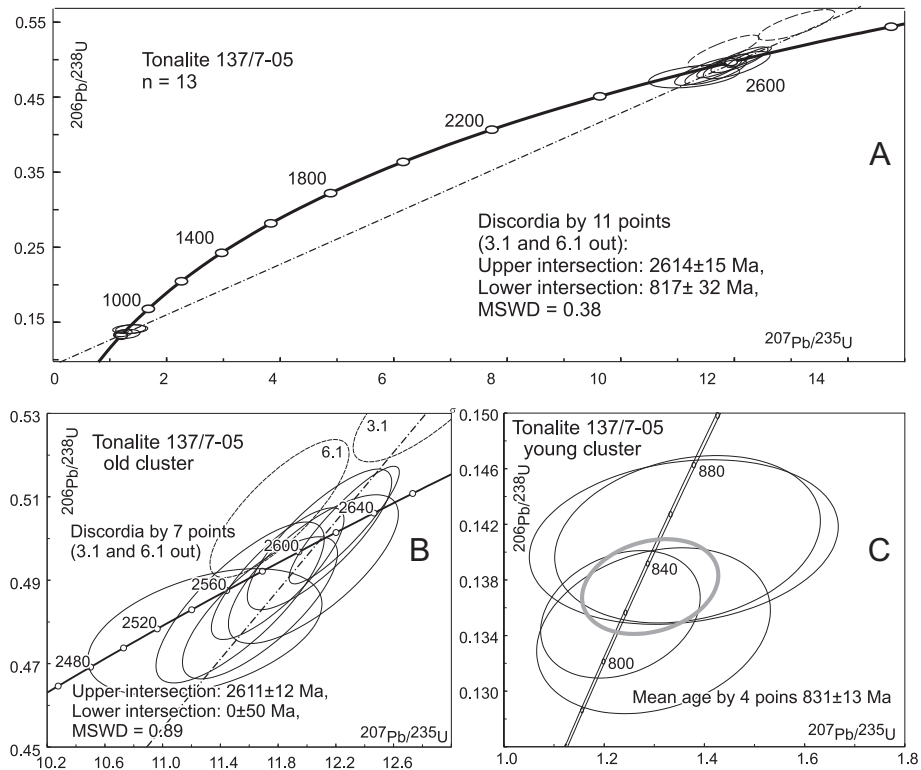


Fig. 15. Concordia diagrams for zircons from tonalite sample 137/7. Error ellipses are 2σ . (A) All points. (B) Old cluster. (C) Young cluster.

831 ± 13 Ma (Fig. 15C). This date is accepted as the likely age of a metamorphic event. However, the number of analyses is insufficient for confident dating, and real metamorphic age may be closer to the upper age limit.

The most reasonable interpretation of the above data is that the core ages correspond to magmatic tonalite crystallization. The ages of low-Th zircon rims indicate new zircon growth during the ca. 831 Ma metamorphic event.

4. Do the Archaean rocks in Transangaria show any specific metamorphic features?

Our study indicates that Archaean rocks do exist in Transangaria. However, they were only found in an outcrop of less than 300 m in length. In fact, the above Archaean block is a large boudin within relatively low-grade metamorphic rocks of unknown age. The question is whether this Archaean block retains any features

Table 3
U and Pb isotopic data for zircons of tonalite 137/7-05. Four upper analyses are for rims, others for cores

Point No.	% ²⁰⁶ Pb _c	ppm U	ppm Th	²³² Th/ ²³⁸ U	ppm ²⁰⁶ Pb*	(1) Age (Ma) by $\frac{^{206}\text{Pb}}{^{238}\text{U}}$	(1) Age (Ma) by $\frac{^{207}\text{Pb}}{^{235}\text{U}}$	(1) $\frac{^{207}\text{Pb}^*}{^{206}\text{Pb}^*}$	±%	(1) $\frac{^{207}\text{Pb}^*}{^{235}\text{U}}$	±%	(1) $\frac{^{206}\text{Pb}^*}{^{238}\text{U}}$	±%	Err corr
137/7-05_6.2	1.50	100	1	0.01	11.7	813 ±14	931 ±150	0.0701	7.1	1.299	7.3	0.1343	1.8	0.247
137/7-05_8.2	0.34	257	3	0.01	30.0	819 ±11	805 ±110	0.0660	5.1	1.232	5.3	0.1355	1.4	0.262
137/7-05_7.2	0.68	107	1	0.01	13.1	849 ±14	929 ±190	0.0700	9.1	1.360	9.3	0.1407	1.7	0.185
137/7-05_4.2	0.73	100	1	0.01	12.2	850 ±14	938 ±160	0.0703	7.7	1.370	7.9	0.1409	1.7	0.220
137/7-05_1.1	0.03	194	186	0.99	79.8	2517 ±27	2572 ±44	0.1715	2.6	11.290	2.9	0.4776	1.3	0.442
137/7-05_7.1	0.26	143	476	3.45	59.5	2542 ±30	2608 ±20	0.1752	1.2	11.670	1.9	0.4834	1.4	0.766
137/7-05_8.1	0.13	105	120	1.18	43.6	2548 ±34	2583 ±21	0.1726	1.3	11.540	2.1	0.4847	1.6	0.788
137/7-05_9.1	0.13	166	321	2.00	70.1	2577 ±28	2597 ±15	0.1740	0.9	11.800	1.6	0.4916	1.3	0.825
137/7-05_4.1	0.12	112	230	2.14	47.3	2582 ±31	2628 ±22	0.1773	1.3	12.040	2.0	0.4927	1.5	0.740
137/7-05_2.1	0.05	132	219	1.72	56.7	2613 ±30	2610 ±16	0.1754	0.98	12.090	1.7	0.4998	1.4	0.816
137/7-05_5.1	0.05	676	766	1.17	292.0	2628 ±25	2622 ±9	0.1767	0.56	12.260	1.3	0.5032	1.1	0.899
137/7-05_6.1	0.06	119	353	3.06	52.1	2653 ±38	2538 ±19	0.1680	1.2	11.790	2.1	0.5092	1.7	0.833
137/7-05_3.1	0.16	102	164	1.65	47.8	2797 ±35	2598 ±21	0.1742	1.3	13.040	2.0	0.5432	1.5	0.769

Errors are 1σ; Pb_c and Pb* indicate the common and radiogenic portions, respectively. (1) Common Pb corrected using measured ²⁰⁴Pb.

indicating its original high-grade metamorphic conditions and is it possible to distinguish such domains among all the metamorphic rocks in Transangaria.

Specialised studies of metamorphism have not been conducted in the investigated area. Nonetheless, we have sufficient data to define differences in PT conditions of metamorphism for various sites and to obtain preliminary PT data. Using an X-ray microprobe and an electron microscope with an energy dispersion unit (equipment of Geological institute SB RAS, Ulan-Ude), the following mineral associations were analysed: garnet–two mica metapelite (samples 131/1, 131/3, 132/1 and 137/1), garnet–biotite metatonalite (137/13) and garnet–biotite amphibolite (137/5, 132/12) from the Ploski-Ostyatski site, garnet–two mica schist (122/1) and garnet–biotite amphibolite (128/4) from the Proklyataya River, and garnet–staurolite–biotite–muscovite schist (39/2) from the Vyatka site. Corresponding sampling locations are shown in Figs. 5, 9 and 11. Representative analyses of the most informative minerals are provided in Tables 4 and 5. An attempt to use the TERMOCALC software (Holland and Powell, 2011) was unsuccessful because alumina polymorphs are lacking in the metapelites and also perhaps due to re-equilibration of the system in the course of multiple metamorphic events. However, the use of a Grt–Bt–Mus–Pl geothermobarometer (Ghent and Stout, 1981) yielded similar PT-values for samples 131/1, 131/3 and 137/1, i.e., three of the four analysed metapelite samples (association Grt + Bt + Mus + Chl + Pl + Qtz) collected from the narrow zone between the Plotsky and Ostyatski brooks, namely $T = 520\text{--}550\text{ }^\circ\text{C}$ and $P = 7\text{--}8\text{ kbar}$. Temperatures were calculated using the biotite–garnet thermometer of Kleemann and Reinhardt (1994), and deviations from the above temperatures did not exceed 10 °C for each sample. Garnet rim compositions were used for the estimates. It should be noted that there is no zoning (either prograde or retrograde) in the garnets, whereas replacement of early garnet by later garnet was observed (Fig. 12C and D), and such replacement may be due to a later phase of metamorphism. Compositional zoning is insignificant in some metapelite garnets, though clear and contrasting prograde zoning is revealed in samples 132/1 and 137/13. A sharp decrease in MnO from core to rim is accompanied by a slight increase in MgO, whereas CaO may either increase or decrease. In one case (sample 132/1), the CaO content sharply decreases and indicates a drop in pressure. In another case (tonalite), CaO significantly increased. The most likely explanation is that the rocks underwent several metamorphic events, and the compositions of the central and marginal parts of garnet may differ due to growth zoning, as well as overgrowth of early metamorphic garnet by new garnet. The metabasites distinctly demonstrate at least two phases of

metamorphism (Fig. 12C and D). The earlier phase garnet with higher concentrations of MgO is preserved in central parts of crystals. Garnet with a higher almandine content developed in their marginal parts and in fractures.

A higher estimated pressure for sample 132/1 (11.6–11.8 kbar at $T = 560\text{ }^\circ\text{C}$) was caused by the presence of low-Ca plagioclase (almost pure albite). The estimate may indicate maximum parameters of metamorphism, but it seems most likely that this was caused by albitisation of primary plagioclase along with preservation of the garnet composition. In other samples, plagioclase is oligoclase–andesine.

Similar estimates ($T = 560\text{ }^\circ\text{C}$ and $P = 8.8\text{ kbar}$) were obtained for the tonalite, suggesting its pre-metamorphic emplacement. However, this case is ambiguous because of the presence of two plagioclase phases, namely, oligoclase and albite (see Table 4). This is not due to albitisation, because both varieties occur as large homogeneous grains. Besides, the above estimates were obtained for oligoclase, whereas for albite the pressure would be as high as 10.6–11 kbar.

Unfortunately, no pressure could be estimated for metapelites from the Vyatka and Proklyataya sites because there was no plagioclase in the analysed thin sections. However, the temperatures calculated by the biotite–garnet thermometer according to Kleemann and Reinhardt (1994) were somewhat higher (560–620 °C).

High-pressure conditions for metamorphic rocks exposed on the Yenisei bank in the vicinity of the Ploski and Ostyatski outlets are also indicated by unusual compositions of garnet, the mineral that is most resistant to retrograde changes and often demonstrates features of syn-deformational growth (Fig. 12B). High contents of Ca in garnet (22–33%, see Table 4) are not typical of metapelites formed under low and moderate pressures. In garnet amphibolites from the same site, the X_{Grs} amounts to 0.44 in the central part and 0.33 at the rim. Such high concentrations of Grs mineral are only observed in eclogites of eclogite–blueschist assemblages (Dobretsov, 1974). Garnets from the Proklyataya River as well as those of the Vyatka site are completely different in composition (see Table 4). The Grs content reaches 6–12% in garnets from metapelites and 17–20% in garnets from metabasites, which is typical of metamorphism at low and moderate pressures.

One more indicator of different metamorphic pressures may be the composition of white mica (Table 5). In contrast to the Proklyataya and Vyatka Rivers, the metapelites at the Ploski-Ostyatski site, contain phengite with higher concentrations of Si, Fe and Mg, which are included in the composition of muscovite according to the isomorphous scheme $2\text{Al} = (\text{Fe}^{2+}, \text{Mg}) + \text{Si}$ (Velde, 1965, 1967).

Table 4
Representative analyses of garnets from metapelite (MP), metabasites (MB) and tonalite (TN).

	Ploskii–Ostyatski										Proklyataya r.				Vyatka					
	131/1 MP		131/3		132/1		137/1		137/13 TN		132/12 MB		137/5		122/1 MP		128/4 MB		39/2 MP	
	c	r	c	r	c	r	c	r	c	r	e	l	e	l	c	r	e	l	c	r
SiO ₂	37.53	36.93	35.28	37.29	36.68	36.48	37.25	36.99	36.88	37.44	37.41	37.47	37.91	37.30	36.38	36.44	38.38	37.40	37.31	36.45
TiO ₂	0.00	0.00	0.00	0.00	0.00	0.00	0.00	0.00	0.00	0.00	0.00	0.00	0.00	0.00	0.00	0.00	0.00	0.00	0.00	0.00
Al ₂ O ₃	20.45	20.35	20.14	20.14	19.70	19.44	20.84	19.93	19.95	20.35	21.10	21.22	20.48	20.46	20.64	20.46	21.07	20.68	20.48	20.50
FeO	30.44	29.01	31.70	30.36	25.42	36.83	26.86	29.80	27.38	27.75	23.58	28.52	26.64	27.50	34.92	37.15	25.64	29.57	34.16	35.83
MnO	1.08	0.83	0.89	0.89	9.48	0.48	0.61	1.87	6.95	3.20	1.87	0.48	1.18	2.31	0.90	1.02	4.02	4.49	0.80	0.57
MgO	1.71	1.76	1.03	1.82	0.50	1.92	2.79	0.66	1.14	1.29	0.93	1.06	3.12	1.59	2.29	2.31	5.04	2.49	3.57	3.13
CaO	8.83	9.35	8.77	8.66	7.64	3.53	11.00	9.61	7.51	10.20	15.52	11.58	10.35	10.20	3.62	2.04	6.43	5.94	3.65	1.79
Na ₂ O	0.00	0.00	0.00	0.00	0.00	0.00	0.00	0.00	0.00	0.00	0.00	0.00	0.00	0.00	0.00	0.00	0.00	0.00	0.00	0.00
K ₂ O	0.00	0.00	0.00	0.00	0.00	0.00	0.00	0.00	0.00	0.00	0.00	0.00	0.00	0.00	0.00	0.00	0.00	0.00	0.00	0.00
Total	100.04	98.23	97.81	99.16	99.42	98.68	99.35	98.86	100.03	100.41	100.41	100.33	99.83	99.49	98.75	99.42	100.58	100.57	99.97	98.27
Si	3.002	2.999	2.903	3.008	2.991	3.001	2.958	3.011	2.982	2.989	2.946	2.976	3.001	2.994	2.971	2.971	2.996	2.980	2.987	2.986
Ti	0.000	0.000	0.000	0.000	0.000	0.000	0.000	0.000	0.000	0.000	0.000	0.000	0.000	0.000	0.000	0.000	0.000	0.000	0.000	0.000
Al	1.928	1.948	1.954	1.915	1.894	1.885	1.951	1.913	1.902	1.915	1.959	1.987	1.911	1.936	1.987	1.967	1.939	1.943	1.933	1.980
Fe ³⁺	0.068	0.055	0.240	0.068	0.125	0.113	0.133	0.065	0.133	0.106	0.150	0.061	0.088	0.076	0.071	0.091	0.068	0.096	0.093	0.047
Fe ²⁺	1.968	1.915	1.942	1.980	1.608	2.421	1.651	1.964	1.718	1.747	1.402	1.833	1.676	1.769	2.313	2.442	1.606	1.874	2.194	2.407
Mn	0.073	0.057	0.062	0.061	0.655	0.033	0.041	0.129	0.476	0.216	0.125	0.032	0.079	0.157	0.062	0.070	0.266	0.303	0.054	0.040
Mg	0.204	0.213	0.126	0.219	0.061	0.235	0.330	0.080	0.137	0.153	0.109	0.125	0.368	0.190	0.279	0.281	0.586	0.296	0.426	0.382
Ca	0.757	0.813	0.773	0.749	0.667	0.311	0.936	0.838	0.651	0.873	1.309	0.985	0.878	0.877	0.317	0.178	0.538	0.507	0.313	0.157
Na	0.000	0.000	0.000	0.000	0.000	0.000	0.000	0.000	0.000	0.000	0.000	0.000	0.000	0.000	0.000	0.000	0.000	0.000	0.000	0.000
K	0.000	0.000	0.000	0.000	0.000	0.000	0.000	0.000	0.000	0.000	0.000	0.000	0.000	0.000	0.000	0.000	0.000	0.000	0.000	0.000
Tot	8.000	8.000	8.000	8.000	8.000	8.000	8.000	8.000	8.000	8.000	8.000	8.000	8.000	8.000	8.000	8.000	8.000	8.000	8.000	8.000
Alm	65.6	63.9	66.9	65.8	53.8	80.7	55.8	65.2	57.6	58.4	47.6	61.6	55.8	59.1	77.9	82.2	53.6	62.9	73.4	80.6
Sps	2.4	1.9	2.1	2.0	21.9	1.1	1.4	4.3	16.0	7.2	4.2	1.1	2.6	5.2	2.1	2.4	8.9	10.2	1.8	1.3
Prp	6.8	7.1	4.4	7.3	2.0	7.8	11.2	2.7	4.6	5.1	3.7	4.2	12.3	6.4	9.4	9.4	19.6	9.9	14.3	12.8
Grs	25.2	27.1	26.6	24.9	22.3	10.4	31.6	27.8	21.8	29.2	44.5	33.1	29.3	29.3	10.7	6.0	18.0	17.0	10.5	5.3
X _{An}	0.31		0.30		0.05		0.21		0.02	0.22	0.37		0.23		No Pl		0.24		No Pl	

Remarks: c – core, r – rim, e – early, l – late. X_{An} – for associated plagioclase. Numbers of samples are the same as in Fig. 9 and 11.

Table 5
Representative analyses of white micas. Numbers of samples are the same as in Figs. 8 and 10.

	Ploski–Ostyatski			Proklyataya		Vyatka	
	131/1	132/1	131/3	137/1	137/13	122/1	39/2
SiO ₂	47.94	48.07	47.39	48.18	48.94	46.30	45.78
TiO ₂	0.72	0.42	0.00	0.58	0.72	0.47	0.55
Al ₂ O ₃	32.29	29.63	31.06	30.10	28.63	34.14	34.88
FeO	1.39	4.41	1.74	2.74	3.11	1.48	1.21
MnO	0.00	0.00	0.00	0.00	0.00	0.00	0.00
MgO	1.67	1.79	2.19	2.22	2.37	0.51	0.93
CaO	0.00	0.00	0.00	0.00	0.00	0.00	0.00
Na ₂ O	0.71	0.97	0.54	0.30	0.43	2.35	1.37
K ₂ O	10.80	10.62	10.64	11.24	11.01	8.55	9.87
Total	95.52	95.91	93.56	95.36	95.21	93.80	94.59
Si	3.190	3.239	3.223	3.241	3.299	3.117	3.069
Ti	0.036	0.021	0.000	0.029	0.037	0.024	0.028
Al	2.533	2.354	2.490	2.387	2.275	2.709	2.757
Fe ²⁺	0.077	0.248	0.099	0.154	0.175	0.083	0.068
Mn	0.000	0.000	0.000	0.000	0.000	0.000	0.000
Mg	0.166	0.180	0.222	0.223	0.238	0.051	0.093
Ca	0.000	0.000	0.000	0.000	0.000	0.000	0.000
Na	0.092	0.127	0.071	0.039	0.056	0.307	0.178
K	0.917	0.913	0.923	0.965	0.947	0.734	0.844
Tot	7.011	7.082	7.029	7.038	7.028	7.025	7.036

Phengite is typical of low-temperature (greenschist- to low amphibolite facies) metamorphism and metamorphism at increased pressure (Fleet, 2003). The highest contents (Si = 3.2–3.6) are typical of metamorphism at high pressure (Velde, 1965, 1967; Dobretsov, 1974; Fleet, 2003); a maximum Si content was recorded in the analyses of phengite from metatonalite sampled at the Ostyatski site (Si = 3.3, Mg + Fe = 0.5).

The above data demonstrate that the Archaean rocks do not preserve any primary mineral compositions that would suggest a possible granulite-facies history. Though the Archaean rocks show some specific features, e.g., amphibolites are mostly composed of bluish-green hornblende in contrast to the younger nearby amphibolites composed of actinolite. These results reflect chemical rather than metamorphic differences. Instead of Archaean metamorphic features, our study revealed a young high pressure/moderate temperature metamorphism in rocks along the Yenisei bank from the Ploski brook outlet to the Vasiliev brook (Fig. 9C) and most likely farther north. In this area, the PT parameters are almost uniform in rocks of different age, including the Archaean block, its Mesoproterozoic (?) and Neoproterozoic metasedimentary cover, as well as the late Neoproterozoic Isakovka metapelite and metabasite. These findings indicate that the high-pressure event is late Neoproterozoic in age and was most likely caused by thrusting of the Isakovka terrane. In contrast, the other studied sites in the Vyatka region and along the Proklyataya River, show metamorphism characterised by moderate or low pressures. As a whole, the mineral compositions of all studied rocks show complete Neoproterozoic overprinting, and our study did not reveal any criteria to distinguish between Archaean and post-Archaean rocks.

5. Main phases of magmatism and metamorphism in Transangaria

5.1. Summary of the geochronological data on the Vyatka site

In addition to the Archaean age, we recognised at least three Neoproterozoic thermal events in rocks of the Yenisei side of Transangaria between 900 and 750 Ma. This by-product of our study is important for the tectonic history of the Yenisei Ridge, which is briefly reviewed below, along with similar ages obtained by other researchers. Migmatization at ca. 900 Ma (age of zircon

cores in sample 11/2-05) was the earliest recognisable event (see Section 2.2). A similar isotopic age was found in zircons from a blastomylonitic gneiss sampled from the middle course of the Gar-evka River (Fig. 4). The dated rock was correlated with gneisses from the Vyatka site (Kozlov et al., 2012). Individual ²⁰⁶Pb/²³⁸U ages range from 901 ± 15 to 860 ± 14 Ma. A concordant age of 882 ± 8 Ma was calculated for a cluster including 11 analyses.

The next event at ~830 Ma was recognised in both study areas (Vyatka and Ostyatski), and in both cases it was the age of metamorphic rims on zircons with low Th/U ratios. The event was also recorded in unzoned zircons from pegmatite sample 11/3-05. We attribute these data to formation of K-feldspar augen-gneiss and blastomylonite in the course of shearing accompanied by heating and potassium metasomatism. Our data are insufficient to confidently constrain the time interval of the process. Based on the assumption that pegmatites were emplaced during the final phase of shearing at ca. 800 Ma ago, the entire affair would have lasted for about 30 Ma.

The last dated event at 770 Ma was the intrusion of granite, comparable to A-type plutons that are widespread in Transangaria (e.g. Vernikovskaya et al., 2003, 2007). This dating was confirmed by Likhanov et al. (2013) from the same Vyatka region, who also found a younger intraplate granite (748 ± 8 Ma, see end of Section 2.2).

Therefore, three episodes of metamorphism and granite emplacement, namely migmatization at 900–880 Ma, shearing and augen-gneiss formation at 830–800 Ma, and A-granite emplacement at 770–750 Ma have been recognised in western Transangaria. It should now be clarified how these ages correlate with the established events on the other part of Transangaria.

5.2. Towards consolidation of the available age data for Transangaria

To clarify what is really known on the age of granitoids and metamorphic rocks in Transangaria we compiled a database including all available zircon U–Pb isotopic ages. These ages are derived using the SIMS and ID TIMS techniques. The data of Volobuev et al. (e.g. 1976) are regarded as incorrect and were not included in the database. We also did not review the geochronological results obtained by other techniques such as CHIME dating of monazite and ³⁹Ar–⁴⁰Ar isotope analyses. The above isotopic systems are less resistant to thermal effects, and the results should be studied together with metamorphic mineral equilibria. As demonstrated above, even the most stable U–Pb isotope system in zircon shows variable loss of radiogenic Pb under local conditions of the Yenisei side of Transangaria that has repeatedly been subjected to thermal impacts. The zircon U–Pb ages for Transangaria discussed below were taken from publications that contain the original analytical data.

The available ages for individual zircon analyses are presented below as histograms where age ranges for each dated object are much wider in comparison to ages calculated as weighted means or concordia ages. However, the selected method is representative as the analyses of relict cores, xenocrysts and detrital grains can be taken into account. The ages calculated from ²⁰⁷Pb/²⁰⁶Pb ratios for all ID TIMS data and for SIMS analyses that are older than 1.0 Ga were used in histogram as more accurate for 1.4–1.0 Ga interval, and more precise for ages older than 1.4 Ga (see Gehrels, 2012 for explanation). Ages based on ²⁰⁶Pb/²³⁸U ratio were used for concordant SIMS data younger than 1.0 Ga for the same reason. The software of Ludwig (2003) and Vermeesch (2012) was used for data presentation.

The result of our compilation is shown in Fig. 16. It is obvious that almost all dated zircons from Transangaria are Neoproterozoic in age. The majority of analyses were performed on granitoids, and this is indicative of a fundamental difference between the

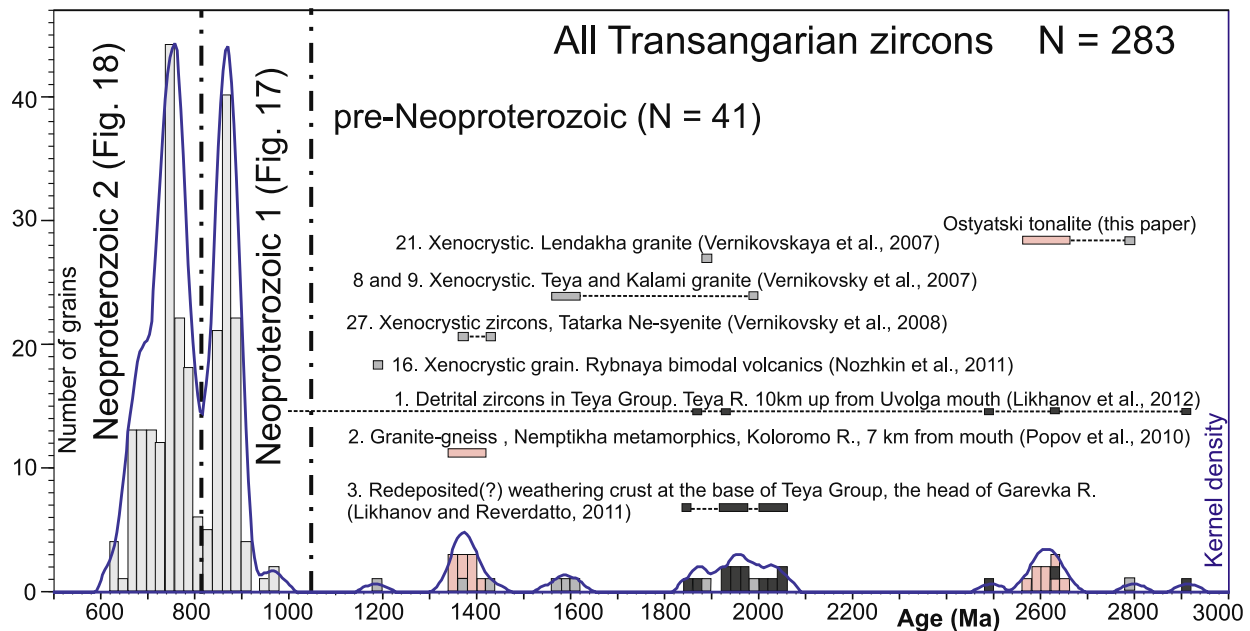


Fig. 16. Histograms for Precambrian zircons found in Transangaria, Yenisei Ridge. Blue curve is a statistical age distribution plotted as 'kernel density estimation' by Vermeesch (2012). Host rocks and references are indicated above the histogram. References are numbered with numbers corresponding to those in Fig. 3. References for pre-Neoproterozoic zircons are indicated. (For interpretation of the references to colour in this figure legend, the reader is referred to the web version of this article.)

Angara-Kan and Transangarian parts of the Yenisei Ridge (see Fig. 2), namely Palaeoproterozoic granitoids are dominant in the former, whereas Neoproterozoic granitoids are dominant in the latter. The Neoproterozoic zircons from Transangaria define two large groups with a boundary at ca. 800 Ma, which are further displayed using separate diagrams (Figs. 17 and 18) at a larger scale.

5.3. Pre-Neoproterozoic zircons

The available data are limited to 41 analyses (Fig. 16), mainly obtained from three samples. The oldest cluster around 2600 Ma is for the Ostyatski tonalite discussed above. One analysis of detrital zircon from the Teya Group falls in the same cluster.

The next age cluster includes late Palaeoproterozoic zircons in the age range 1850–2050 Ma. Most of this cluster is composed of zircons from sillimanite schists sampled from the Karpinsky Ridge Formation (Teya Group) (Likhonov and Reverdatto, 2011). These authors suggested that the schist protolith was a kaolinite clay transported from the Siberian platform into a marine basin. Marine clayey sediments typically do not contain 200 μm -zircons. Sample was collected at the base of Teya Group, which unconformably overlies older metamorphic rocks mapped as Nemtikha and Malogarevka units. It seems likely that the original sediment may represent the weathering crust washed out from adjacent uplands composed of older granitic and metamorphic rocks. The remaining analyses in this cluster are xenocrystic grains captured by Neoproterozoic granite melts and several detrital zircons from Teya Group metasediments (Fig. 16). Overall, the cluster corresponds in age to rocks that constitute the Angara-Kan block and are typical of the Siberian craton.

The age of the youngest pre-Neoproterozoic cluster is ~1350–1400 Ma. The majority of zircons was extracted from granite-gneiss sampled from the Nemtikha metamorphic complex (Fig. 3) (Popov et al., 2010). It was suggested by these authors that the protolith was a felsic igneous rock with an intraplate setting. The last statement is based on the presence of amphibolite within the surrounding gneisses, which may constitute a bimodal association

in combination with the dated rock. The cluster also includes two xenocrystic grains from the Tatarka nepheline syenite (Vernikovskiy et al., 2008). These findings may indicate that Mesoproterozoic magmatism was not a local phenomenon but was presented throughout Transangaria.

The other pre-Neoproterozoic zircon ages are represented by solitary analyses. Three analyses constitute a group with an age of ~1600 Ma and were obtained from one xenocryst, and thus also represent a single age. The age range from 1000 to 1300 Ma, which corresponds to the Grenville orogeny, is only represented by one grain. This is a xenocryst from the Neoproterozoic Rybnaya rhyolite (Fig. 16).

5.4. The early Neoproterozoic (1000–800 Ma)

The early Neoproterozoic (1000–800 Ma) dataset confirms our conclusion that a Grenville-age orogeny is not manifested in Transangaria. The age interval 950–1000 Ma is represented by two detrital zircons from the Teya Group and one xenocrystic grain from a rhyolite (Fig. 17).

Most early Neoproterozoic ages plot in the 905–840 Ma range (Fig. 17), including gneissic granites widespread in the centre of Transangaria. These granite bodies were interpreted by Nozhkin et al. (1999) as granite-gneiss domes and classified as synmetamorphic and synkinematic. The age distribution in Fig. 17 denotes a culmination of igneous activity at 875 Ma and subsidiary peaks at ~895 and ~860 Ma. It is unlikely that the age peaks correspond to distinct phases of magmatic activity. Looking at the curve, we suggest that granite production was most intense during the period 885–855 Ma. The dataset indicates that granites of this age are common in central Transangaria but also occur along its western part adjacent to the Yenisei River. The earliest phase is more clearly documented in the latter region (Fig. 17). In western Transangaria, however, such granites do not form distinct mappable bodies and are represented either by migmatites or blastomylonitised granite gneisses with vague contacts.

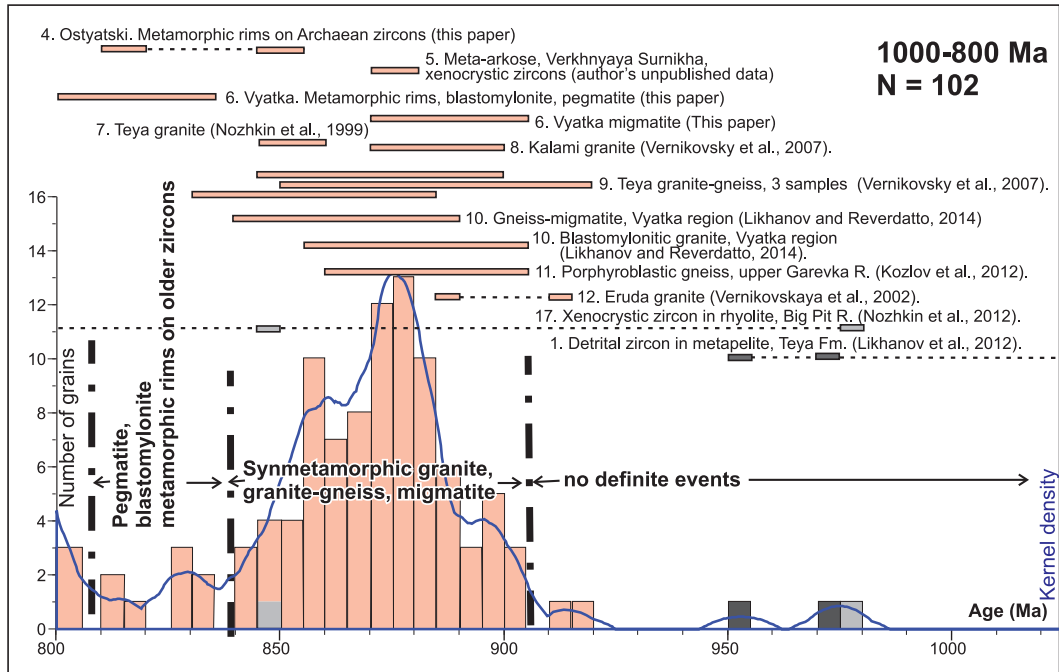


Fig. 17. Zircon age data for the 1000–800 Ma interval (see caption of Fig. 16 for explanation). (See above-mentioned references for further information.)

The formation of blastoporphyritic gneisses and associated pegmatites continued into the middle Neoproterozoic. This younger age interval of 830–800 Ma is mostly represented by our data, which are insufficient to define a distinct age spike in the plot (see Fig. 17). It seems that this event is specifically manifested in western Transangaria, where it is confirmed by the age of metamorphic rims around older zircon crystals at both of our studied sites.

5.5. The late Neoproterozoic

The late Neoproterozoic era represents more tectonic events and corresponding magmatic activity than the earlier periods. Most dated zircons come from the Glushikha granite association, including numerous cross-cutting bodies that are abundant in Transangaria (Figs. 18 and 3). The largest body in our study area

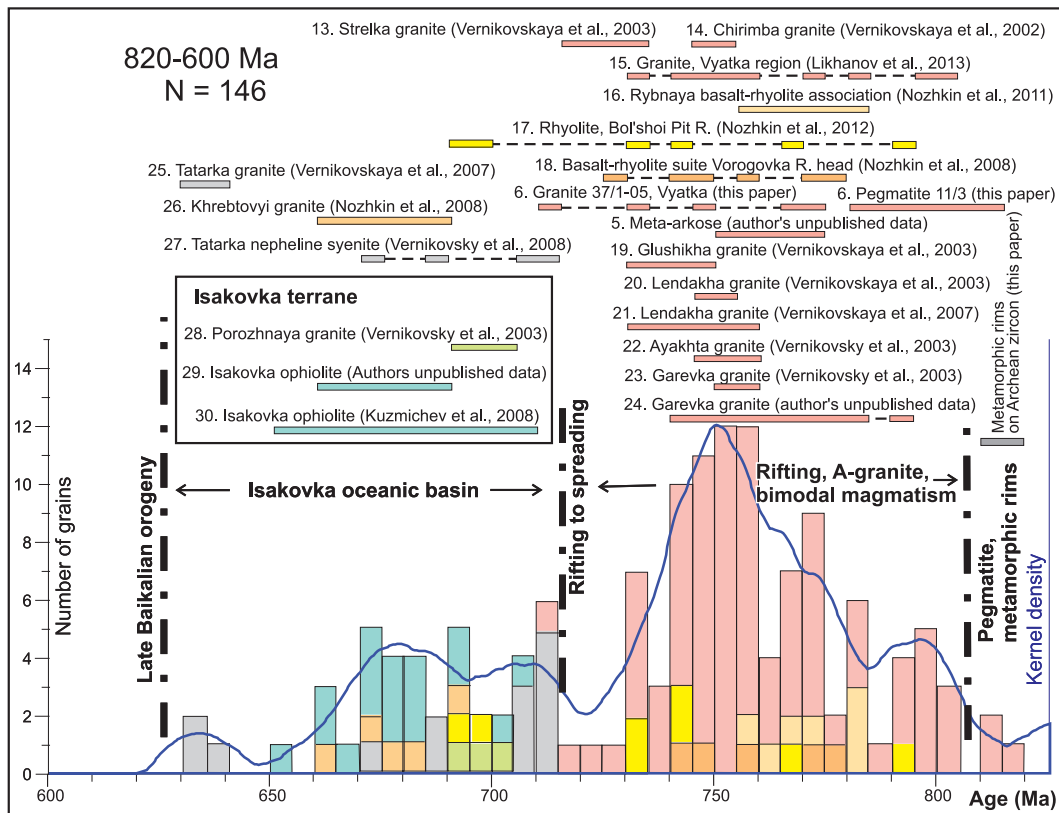


Fig. 18. Zircon age data for the 820–600 Ma range (see caption for Fig. 16 for explanation).

is the Garevka pluton (Fig. 4), a single-phase A-type granite intrusion of uniform composition and resembling a rapakivi granite (Kuzmichev, 1987). In almost every sample, accessory fluorite can be found. Some granites of this age group are not included in the Glushikha suite due to different compositions. Among these is the well-known Ayakhta pluton (#21 in Fig. 3), located in the eastern part of Transangaria in the vicinity of the inferred suture between the Central-Angara and Western-Angara “terrane” of Vernikovskiy et al. (2003, 2007). Most granites intruded at 775–740 Ma with peak activity at 750 Ma. The Glushikha magmatism lasted at least up to 718 ± 9 Ma (Strelka pluton, ID TIMS; Vernikovskaya et al., 2003).

The Glushikha granites are either interpreted as post-collisional (Vernikovskaya et al., 2007) or intraplate, possibly related to a mantle plume (Nozhkin et al., 2008). Intraplate rift-related magmatism is supported by the presence of bimodal basalt-rhyolite volcanic associations of the same age, which are found in different parts of the Yenisei Ridge (Nozhkin et al., 2008). The age bins for felsic members of these associations are marked in Fig. 18 using special colours.

We suggest that at some point in time, rifting in the western Yenisei Ridge gave way to spreading and formation of the Isakovka oceanic basin. In Fig. 18 this event is inferred to have occurred at 720 Ma; however, it could also have occurred earlier. The youngest group of Neoproterozoic zircons (710–650 Ma) is represented by the Isakovka oceanic gabbro and island-arc granitoids (blue and green colours in Fig. 18). At the same time, intraplate alkaline magmas intruded into the continental side of the Yenisei Ridge. Such magmatic activity went on even later (Fig. 18).

6. Precambrian evolution of Transangaria

The above zircon age database enables us to verify published models on the evolution of the Yenisei Ridge and leads to new conclusions. Our proposed sequence of geological events did not take into account the sedimentary record because reliable age data on stratified successions are lacking with the exception of the uppermost units.

6.1. Pre-Neoproterozoic basement

The early Precambrian rocks were found at three sites, which reveal three igneous or metamorphic episodes: Neoproterozoic (2.6 Ga), Palaeoproterozoic (2050–1850 Ma) and Mesoproterozoic (1350–1400 Ma). The 2050–1850 Ma episode is most important for comparison with the basement of the Siberian craton. This basement crops out in the Angara-Kan block, which is predominantly composed of the Palaeoproterozoic metamorphic rocks (Bibikova et al., 1993; Turkina et al., 2012; Urmantseva et al., 2012). The available zircon data are insufficient to conclude that Transangaria is underlain by early Precambrian basement. The more convincing are Nd isotopic data for Neoproterozoic granitoids and felsic volcanics. Reported Nd model ages for them are mostly Palaeoproterozoic in range of 1.7–2.1 Ga with occasional Mesoproterozoic and Neoproterozoic values (Nozhkin et al., 2008, 2012; Popov et al., 2010; Vernikovskaya et al., 2002, 2003, 2009; Vernikovskiy et al., 2003, 2007). Nd isotopic systematic does not directly indicate an age of basement, due to different crustal metaigneous and metasedimentary sources for Neoproterozoic felsic melts. Besides the sources for A-type granites and volcanics might also include mantle component (Nozhkin et al., 2008; Vernikovskaya et al., 2009). However that may be, the Nd isotopic model ages are rather uniform, and Transangaria as a whole may be interpreted as a region with Palaeoproterozoic basement, which include Neoproterozoic domains.

6.2. Did a Grenville-age orogeny really occur at the Yenisei Ridge?

Some published reports attempted to justify the common occurrence of granitoids and metamorphic rocks with ages of 1200–900 Ma in Transangaria, corresponding to a Grenville-age orogeny, which was interpreted as possible connection between Siberia and the Rodinia supercontinent (Nozhkin et al., 2011; Likhanov et al., 2012, 2014, 2015 and references therein). Our review of the isotope data does not support these ideas because 900–1200 Ma zircons are lacking in the dataset. This conclusion is important for the interpretation of Yenisei Ridge geology. The lack of a Grenville-age event does not prove that Siberia was not part of Rodinia at the Mesoproterozoic and Neoproterozoic boundary because Siberia could have become part of the supercontinent during more ancient times. An important fact is that Transangaria does not differ from the rest of the Siberian craton where a Grenville-age orogeny has not been detected (e.g., Gladkochub et al., 2010). Moreover, if the proposed age of the sedimentary sequences on the Yenisei Ridge is correct, the western margin of the Siberian platform can be inferred to have developed as a passive margin during the latest Mesoproterozoic and earliest Neoproterozoic (Fig. 19A).

6.3. Early Neoproterozoic orogeny: what collided with what?

We infer that voluminous granite magmatism (considered as synmetamorphic, syncollisional and synkinematic) at 900–840 Ma reflects a collisional event or a series of consecutive events. There is no generally accepted opinion on the tectonic interpretation of this collision. For example, Nozhkin et al. (2011) suggested that the event reflects amalgamation of Siberia with Rodinia during the final phase of its assembly. Vernikovskiy et al. (2007 and references therein) proposed that Transangaria was a separate microcontinent that drifted apart from Siberia, and the specific causes of magmatism was not an issue for these authors. They placed the time of collision between this assumed exotic terrane and Siberia at 760–720 Ma (see Section 6.4).

We propose a different model. Syncollisional granitoids (900–840 Ma) are common throughout the major part of Transangaria, including the western Yenisei-side zone. The simplest and most obvious assumption is that the orogeny during the first half of the Neoproterozoic resulted from collision of an unspecified terrane with the western margin of the Siberian craton (Fig. 19B). We suggest that this collided terrane is no longer present in the structure of the Yenisei Ridge. This model explains several phenomena typical of the western part of the Ridge. First, migmatites and granite-gneisses in this area formed earlier than the Teya granite-gneiss domes in the central part of the Ridge. Therefore, this process may have begun in the western part of the Ridge. Second, synmetamorphic shearing (with a supposed age of 830–800 Ma) in western Transangaria is an indirect indication that this side of the Yenisei Ridge was in contact with some unknown continental landmass in the mid-Neoproterozoic. Third, the only known detrital zircon ages for sedimentary units of Transangaria are for lower Neoproterozoic (?) sandstone (Pogoryui Formation) (Powerman et al., 2013). Their sample was dominated by Mesoproterozoic zircons whose source cannot be found in Siberia. It seems plausible that the inferred exotic terrane may be the source of such exotic zircons if we could ever prove that Pogoryui Fm. is of appropriate age (now it is thought to be Mesoproterozoic).

Augen-gneisses, mylonites and blastocataclases can be traced along the Yenisei side of Transangaria and represent the deep section of a high-temperature shear zone, accompanied by K-metasomatism. Augen-gneisses of the Yenisei Ridge are similar to blastomylonites of the marginal shear zone dividing the Siberian craton and younger terranes attached to it in the Ol'khon region, Baikal (Fedorovsky et al., 2010). We suggest that the blastomy-

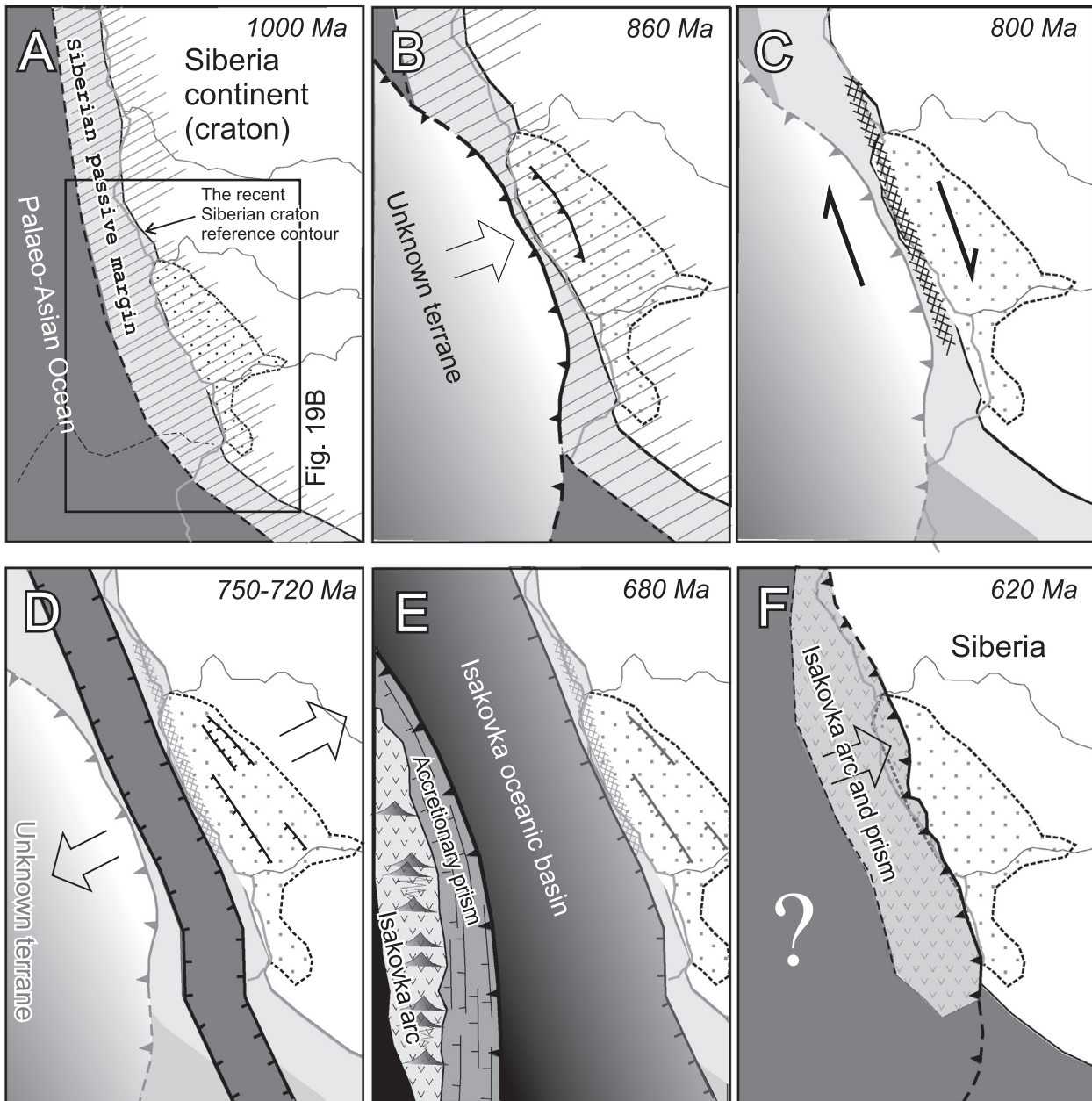


Fig. 19. Speculative cartoons for six successive phases of possible Neoproterozoic evolution of the Yenisei Ridge (in modern coordinates). Current position of the Yenisei Ridge is indicated by dotted line; main current rivers are shown for reference. The age window for each picture is indicated in the top right corner. (A: 1000 Ma) Western passive margin of the Siberian craton; no Grenville-age orogeny. (B: 860 Ma) Collision of unknown terrane with margin of Siberian craton. (C: 800 Ma) Counterclockwise rotation of Siberian craton. Blastomylonitic gneiss formation in a shear zone. (D: 750–720 Ma) Rifting and spreading; formation of a new ocean basin. (E: 680 Ma) Isakovka island arc with frontal accretionary prism facing the Siberian margin. (F: 620 Ma) Collision of the Isakovka arc with the Siberian craton; thrusting of accretionary prism and arc rocks onto the Siberian margin.

lonites at the western Yenisei Ridge also reflect a shear zone at the edge of the ancient craton caused by its counter-clockwise rotation (Fig. 19C). This suggestion is tentative and needs to be supported by structural studies and additional age data. Counter-clockwise rotation of Siberian craton at the second third of Neoproterozoic is confirmed by palaeomagnetic evidences (Metelkin et al., 2012).

6.4. Late Neoproterozoic intraplate magmatism in an extensional environment

The first half of the late Neoproterozoic (770–720 Ma) was a time of voluminous emplacement of intraplate Glushikha-type granites as well as basalt-rhyolite bimodal associations. According

to Nozhkin et al. (2008, 2011), this magmatism developed in an extensional environment and was caused by ascent of a mantle plume. This phase of the Yenisei Ridge evolution seems the least questionable. However, collision between the Central Angara terrane (embracing most of Transangaria, Fig. 2) and the Siberian continent was proposed by Vernikovskiy et al. (2007 and references therein) to have occurred at that time. They suggested the Rybnaya-Ishimba fault zone to represent a suture. The zone extends in eastern Transangaria from the Angara River to the northern termination of the Yenisei Ridge (Fig. 2).

Serpentinities and amphibolites, which may represent relics of oceanic crust, occur in the Rybnaya River region (Fig. 3). Nozhkin et al. (2011) were confident that these rocks are not related to

ophiolite but are intraplate high-Ti basalts and picrites. According to Nozhkin et al. (2011), the Rybnaya basalts are associated with rhyolite and form a bimodal association due to rifting. In addition, the Ishimba zone is not a distinct and continuous thrust fault but rather represents a series of en-echelon reverse faults, and serpentinite could not be traced northwards of the Rybnaya River. There is also one additional small serpentinite body, located in the vicinity of the Sukhoi Pit River mouth (Fig. 3), whose origin is unknown. However, it is impossible to trace any boundary along Transangaria (with the exception of the Isakovka boundary) that may be interpreted as a suture.

Therefore, the collision proposed by Vernikovskiy et al. (2003, 2007) for the time interval 760–720 Ma is poorly documented and unlikely to have occurred. The alternative model of Nozhkin et al. (2008, 2011) for an extensional setting in Transangaria appears to be better argued. We suggest that, due to progressive extension, rifting was followed by spreading. As a result, a fragment of the western margin of the Siberian continent (including the assumed terrane accreted to it during the early Neoproterozoic) was detached from Siberia, and its subsequent fate remains unknown (Fig. 19D). The onset of spreading has not been dated, and this process may have begun at 750–720 Ma or earlier.

6.5. Second half of the late Neoproterozoic: opening and closure of the Isakovka oceanic basin

Extensional processes in the areas to the west (in modern coordinates) of Siberia resulted in the formation of an ocean basin whose remnants are represented by the Isakovka ophiolites (Fig. 2). There are two almost identical ages, 682 ± 13 and 672 ± 6 Ma, for the Isakovka oceanic gabbro, which were interpreted to correspond to the time of sea-floor spreading (Kuzmichev et al., 2008; Kuzmichev, 2009). The marginal part of the Isakovka belt is composed of alternating slices of oceanic crust and metasedimentary rocks (originally mainly flysch) and can thus be interpreted as an accretionary prism.

The polarity of subduction, and at which side of the marginal oceanic basin the prism formed are not known. Volcanic rocks of appropriate age are rare on the continental side of Transangaria, and their suprasubduction origin is uncertain. Thus, it seems more plausible that subduction occurred beneath the island arc that is tentatively shown in Fig. 19E. In this case, the above accretionary prism formed in front of the Isakovka island arc, whose volcanic rocks are exposed in the central part of the Isakovka terrane (Kuzmichev, 1987). In the northwestern part of the terrane, granitoids (#28 in Fig. 3), which are also assumed to be of island-arc origin, were dated at ~ 700 Ma (Vernikovskiy et al., 2003).

Subsequently, the Isakovka island arc collided with the western margin of the Siberian continent, and the Isakovka accretionary prism was thrust onto the Siberian margin (Fig. 19F). Syncollisional granites of this phase were not found in the Yenisei Ridge. We agree with Vernikovskiy et al. (2003), that collision occurred 630–600 Ma ago, although it could have occurred somewhat earlier. Thrusting caused high-pressure metamorphism in our study area (see Section 4). This major event denotes the end of the Precambrian geological history of the Yenisei Ridge. Collision was followed by the formation of synorogenic and postorogenic sedimentary successions at the end of the Precambrian, and these are overlain by Cambrian shallow-water carbonate deposits and evaporites.

7. Conclusions

Our study clarifies some unresolved issues of the Yenisei Ridge geology and provides an outline of the main phases in its evolution.

1. Archaean and Palaeoproterozoic rocks are present in Transangaria, and it is possible that originally this terrain was underlain by early Precambrian continental crust that was strongly reworked during the Neoproterozoic. This conclusion is based on a few samples of old rocks, occasional xenocrystic zircons entrained by granitic melts and on the Nd model ages for granitic and volcanic rocks. The rarity of old zircon in our dataset can be explained by the fact that typically, felsic igneous rocks representing newly-formed melts were collected for zircon dating. A more promising approach to find additional evidence for Palaeoproterozoic or Archaean crust would be to obtain zircons ages from metamorphic schists, which mapped in Transangaria as Nemtikha and Malogarevka units.
2. Evidence for the occurrence of a Grenville-age orogeny in Transangaria was not confirmed by U–Pb zircon geochronological data.
3. We found no evidences that Transangaria is an exotic Neoproterozoic terrain and consider it as a marginal segment of the Siberian craton reworked during Neoproterozoic orogenies. Our interpretation of the Neoproterozoic geological evolution of Transangaria includes the following events.
 - (i) Syntectonic granitoids and migmatites were generated at 900–840 Ma and probably reflect a collision event or a series of events. We suggest that it was a collision of an unknown terrane, located to the west of the present Yenisei Ridge, with the margin of the Siberian continent.
 - (ii) A blastomylonite zone traced along the western Yenisei Ridge provides evidence of high-temperature shearing some 830–800 Ma ago. We suggest that this shearing occurred at the boundary of the Siberian craton and a Precambrian block that was adjacent to its western margin but is no longer present.
 - (iii) The continental block of Transangaria evolved in an extensional environment at 800–700 Ma. Within this period (most likely, closer to its end), rifting changed to spreading, and a continental block was separated from the western margin (in modern coordinates) of the Siberian continent and drifted away. As a result, the Isakovka oceanic basin formed and in the current structure of the Yenisei Ridge, this is represented by the ophiolite of the Isakovka belt, containing slices of oceanic rocks incorporated into an accretionary prism.

The above conclusions are preliminary. The age limits for the each geologic phase seem to be too wide to reflect just one event. Our inferences are mainly based on the available zircon dating. There are also other datasets that were not included in the present review. Among these, the most important are data on the composition and tectonic setting of sedimentary rocks. We did not review such data due to uncertainties on their ages.

Acknowledgements

We are grateful to E.V. Postel'nikov and A.D. Nozhkin, who introduced the first author to the geology of the Yenisei Ridge, to A.N. Larionov and E.N. Lepekhina for SHRIMP II isotope measurements, to S.V. Kanakin for his support with electron-probe microanalyses, to K.E. Degtyarev and M.V. Luchitskaya for reviewing the first version of manuscript and for providing valuable comments and to anonymous reviewers for useful comments. O.M. Turkina and A.A. Storozhenko provided us with recent geological maps of the Yenisei Ridge. Our special thanks to A. Kroener, whose comments and suggestions helped to improve and clarify the manuscript. This study was financially supported by the Russian Foundation for Basic Research (Project 12-05-00229), the Integration Program of the Earth Sciences Section of SB RAS (Project No.

10) and the Program of Department of Earth sciences, RAS 'Structure, composition and formation of continental crust in the Neogeic'.

References

- Belousova, E.A., Griffin, W.L., O'Reilly, S.Y., Fisher, N.I., 2002. Igneous zircon: trace element composition as an indicator of source rock type. *Contrib. Mineral. Petrol.* 143, 602–622.
- Bibikova, E.V., Gracheva, T.V., Makarov, V.A., Nozhkin, A.D., 1993. Age boundaries in the geological evolution of early Precambrian of Yenisei Ridge. *Stratigr. Geol. Correlat.* 1, 35–40 (in Russian).
- Condie, K.C., 1999. Mafic crustal xenoliths and the origin of the lower continental crust. *Lithos* 46, 95–101.
- Dobretsov, N.L., 1974. *Blueschist and Eclogite–Blueschist Complexes of the USSR*, Nauka, Novosibirsk, 430 p. (in Russian).
- Fedorovsky, V.S., Sklyarov, E.V., Izokh, A.E., Kotov, A.B., Lavrenchuk, A.V., Mazukabzov, A.M., 2010. Strike-slip tectonics and subalkaline mafic magmatism in the Early Paleozoic collisional system of the western Baikal region. *Russ. Geol. Geophys.* 51, 534–547.
- Fleet, M.E., 2003. *Rock-forming minerals*, Vol. 3A, Micas. Geological Society of London, 758 p.
- Gehrels, G., 2012. Detrital zircon U–Pb geochronology: current methods and new opportunities. In: Busby, C., Azor, A. (Eds.), *Tectonics of Sedimentary Basins: Recent Advances*. Blackwell, pp. 47–62.
- Ghent, E.D., Stout, M.Z., 1981. Geobarometry and geothermometry of plagioclase–biotite–garnet–muscovite assemblages. *Contrib. Mineral. Petrol.* 76, 92–97.
- Gladkochub, D.P., Donskaya, T.V., Wingate, M.T.D., Mazukabzov, A.M., Pisarsky, S. A., Sklyarov, E.V., Stanevich, A.M., 2010. A one-billion-year gap in the Precambrian history of the southern Siberian Craton and the problem of the Transproterozoic supercontinent. *Am. J. Sci.* 310, 812–825.
- Holland, T.J.B., Powell, D.R., 2011. An improved and extended internally consistent thermodynamic dataset for phases of petrological interest, involving a new equation of state for solids. *J. Metamorph. Geol.* 29, 333–383.
- Kachevsky, L.K., Kachvskaya, G.I., Storozhenko, A.A., Zuev, V.K., Diner, A.E., Vasil'ev, N.F., 1994. On the determination Archean metamorphic complexes at Transangarian part of Yenisei Ridge. *Domestic Geology*, No. 11–12, 45–49 (in Russian).
- Kachevsky, L.K., Kachevskaya, G.I., Grabovskaya, J.M., 1998. Geological Map of Yenisei Ridge, Scale 1:500000. Krasnoyarsk, Krasnoyarskgeols'emka, 6 sheets (in Russian).
- Kleemann, U., Reinhardt, J., 1994. Garnet–biotite thermometry revisited: the effect of Al^{VI} and Ti in biotite. *Eur. J. Mineral.* 6, 925–941.
- Kozlov, P.S., Likhonov, I.I., Reverdatto, V.V., Zinov'ev, S.V., 2012. Tectonometamorphic evolution of the Garevka polymetamorphic complex (Yenisei Ridge). *Russ. Geol. Geophys.* 53 (11), 1133–1149.
- Kusnetsov, Yu.A., 1941. Petrology of the Yenisey Range. Data on geology of Western Siberia, Tomsk, 240 pp. (in Russian).
- Kuzmichev, A.B., 1987. Tectonics of the Isakovka Synclinorium of the Yenisei Ridge. Abstract for PhD Thesis. Moscow Geological Institute Academy of Sciences of USSR, 19 pp. (in Russian).
- Kuzmichev, A.B., 2009. On the Age of Oceanic Metagabbro (Zircon, SHRIMP) of Isakovka Ophiolite Belt (Yenisei Ridge). Geodynamic Evolution of Central Asian Orogenic Belt (from Ocean to Continent). Institute of Earth crust, Irkutsk, vol. 1, pp. 154–155 (in Russian).
- Kuzmichev, A.B., Paderin, I.P., Antonov, A.V., 2008. Late Riphean Borisikha ophiolite (Yenisei Ridge): U–Pb zircon age and tectonic setting. *Russ. Geol. Geophys.* 49, 883–893.
- Lentz, D.R., 1999. Carbonatite genesis: a reexamination of the role of intrusion-related pneumatolytic skarn processes in limestone melting. *Geology* 27, 335–338.
- Likhonov, I.I., Reverdatto, V.V., 2011. Lower proterozoic metapelites in the northern Yenisei Range: nature and age of the protolith and the behavior of material during collisional metamorphism. *Geochem. Int.* 49, 224–252.
- Likhonov, I.I., Reverdatto, V.V., 2014. Geochemistry, age, and petrogenesis of rocks from the Garevka metamorphic complex, Yenisey Ridge. *Geochem. Int.* 52, 1–21.
- Likhonov, I.I., Reverdatto, V.V., Kozlov, P.S., 2012. U–Pb and 40Ar/39Ar evidence for Grenvillian activity in the Yenisey Ridge during formation of the Teya metamorphic complex. *Geochem. Int.* 50 (6), 551–557.
- Likhonov, I.I., Reverdatto, V.V., Popov, N.V., 2013. New data on Late Riphean intraplate granitoid magmatism in the Transangarian Yenisei Ridge. *Dokl. Earth Sci.* 453, 1100–1105.
- Likhonov, I.I., Nozhkin, A.D., Reverdatto, V.V., Kozlov, P.S., 2014. Grenville tectonic events and evolution of the Yenisei Ridge at the western margin of the Siberian craton. *Geotectonics* 48, 371–389.
- Likhonov, I.I., Reverdatto, V.V., Kozlov, P.S., Khiller, V.V., Sukhorukov, V.P., 2015. P–T–t constraints on polymetamorphic complexes of the Yenisey Ridge, East Siberia: implications for Neoproterozoic paleocontinental reconstructions. *J. Asian Earth Sci.* 113, 391–410.
- Liu, Y., Berner, Z., Massonne, H.-J., Zhong, D., 2006. Carbonatite-like dykes from the eastern Himalayan syntaxis: geochemical, isotopic, and petrogenetic evidence for melting of metasedimentary carbonate rocks within the orogenic crust. *J. Asian Earth Sci.* 26, 105–120.
- Ludwig, K.R., 2001. *Squid 1.02*. Berkeley Geochronology Center, Special Publication No. 2.
- Ludwig, K.R., 2003. *ISOPLLOT 3.00*. A Geochronological Toolkit for Microsoft Excel. Berkeley Geochronology Center, Special Publication No. 4.
- Metelkin, D.V., Vernikovskiy, V.A., Kazansky, A.Yu., 2012. Tectonic evolution of the Siberian paleocontinent from the Neoproterozoic to the Late Mesozoic: paleomagnetic record and reconstructions. *Russ. Geol. Geophys.* 53, 675–688.
- Nozhkin, A.D., Turkina, O.M., Bibikova, E.V., Terleev, A.A., Khomentovskiy, V.V., 1999. Riphean granite–gneiss domes of the Yenisei Range: geological structure and U–Pb isotopic age. *Russ. Geol. Geophys.* 40 (9), 1284–1292.
- Nozhkin, A.D., Turkina, O.M., Bayanova, T.B., Berezhnaya, N.G., Larionov, A.N., Postnikov, A.A., Travin, A.V., Ernst, R.E., 2008. Neoproterozoic rift and within-plate magmatism in the Yenisei Ridge: implications for the breakup of Rodinia. *Russ. Geol. Geophys.* 49 (7), 503–519.
- Nozhkin, A.D., Turkina, O.M., Bayanova, T.B., 2009. Paleoproterozoic collisional and intraplate granitoids of the southwest margin of the Siberian craton: petrogeochemical features and U–Pb geochronological and Sm–Nd isotopic data. *Dokl. Earth Sci.* 428, 1192–1197.
- Nozhkin, A.D., Borisenko, A.S., Nevol'ko, P.A., 2011. Stages of Late Proterozoic magmatism and periods of Au mineralization in the Yenisei Ridge. *Russ. Geol. Geophys.* 52, 124–143.
- Nozhkin, A.D., Kachevsky, L.K., Dmitrieva, N.V., 2012. Late neoproterozoic metarhyolite–basalt association of the Glushikha trough (Yenisei Ridge): new data on the petrogeochemical composition, age, and conditions of formation. *Dokl. Earth Sci.* 445, 910–915.
- Popov, N.V., Likhonov, I.I., Nozhkin, A.D., 2010. Mesoproterozoic granitoid magmatism in the Trans-Angara segment of the Yenisei Range: U–Pb evidence. *Dokl. Earth Sci.* 431, 418–423.
- Powerman, V., Shatsillo, A., Chumakov, N., Pavlov, V., Hourigan, J., Kapitonov, I., 2013. Siberian Craton: A Journey from Rodinia to CAOS as Evidenced by Detrital Zircons. Geodynamic Evolution of Central Asian Mobile Belt (from an Ocean to the Continent) (Abstract Volume). Institute of Earth Crust, Irkutsk, pp. 278–283.
- Sklyarov, E.V., Fedorovsky, V.S., Kotov, A.B., Lavrenchuk, A.V., 2013. Carbonate and silicate–carbonate injection complexes in collision systems: the West Baikal region as an example. *Geotectonics* 47, 180–196.
- Sun, S.S., McDonough, W.F., 1989. Chemical and isotopic systematics of oceanic basalts: implications for mantle composition and processes. In: Saunders, A.D., Norry, M.J. (Eds.), *Magmatism in the Ocean Basins*, vol. 42. Geological Society Special Publication, pp. 313–345.
- Turkina, O.M., Berezhnaya, N.G., Lepekina, E.N., Kapitonov, I.N., 2012. Age of mafic granulites from the early Precambrian metamorphic complex of the Angara-Kan terrain (Southwestern Siberian Craton): U–Pb and Lu–Hf isotope and REE composition of zircon. *Dokl. Earth Sci.* 445, 986–993.
- Urmantseva, L.N., Turkina, O.M., Larionov, A.N., 2012. Metasedimentary rocks of the Angara-Kan granulite–gneiss block (Yenisey Ridge, south-western margin of the Siberian Craton): provenance characteristics, deposition and age. *J. Asian Earth Sci.* 49, 7–19.
- Vavra, G., Gebauer, D., Schmid, R., Compston, W., 1996. Multiple zircon growth and recrystallization during polyphase Late Carboniferous to Triassic metamorphism in granulites of the Ivrea Zone (Southern Alps): an ion microprobe (SHRIMP) study. *Contrib. Mineral. Petrol.* 122, 337–358.
- Velde, B., 1965. Phengite micas: synthesis, stability, and natural occurrence. *Am. J. Sci.* 263, 886–913.
- Velde, B., 1967. Si⁴⁺ content of natural phengites. *Contrib. Mineral. Petrol.* 14, 250–258.
- Vermeesch, P., 2012. On the visualisation of detrital age distribution. *Chem. Geol.* 312–313, 190–194.
- Vernikovskaya, A.E., Vernikovskiy, V.A., Sal'nikova, E.B., Datsenko, V.M., Kotov, A.B., Kovach, V.P., Travin, A.V., Yakovleva, S.Z., 2002. Yeruda and Chirimba granitoids (Yenisei Ridge) as indicators of Neoproterozoic collisional events. *Russ. Geol. Geophys.* 43, 245–259.
- Vernikovskaya, A.E., Vernikovskiy, V.A., Sal'nikova, E.B., Kotov, A.B., Kovach, V.P., Travin, A.V., Palessky, S.V., Yakovleva, S.Z., Yasenev, A.M., Fedoseenko, A.M., 2003. Neoproterozoic postcollisional granitoids of the Glushikha complex, Yenisei Ridge. *Petrology* 11 (1), 48–61.
- Vernikovskaya, A.E., Vernikovskiy, V.A., Sal'nikova, E.B., Kotov, A.B., Kovach, V.P., Travin, A.V., Wingate, M.T.D., 2007. A-type leucogranite magmatism in the evolution of continental crust on the western margin of the Siberian craton. *Russ. Geol. Geophys.* 48, 3–16.
- Vernikovskaya, A.E., Vernikovskiy, V.A., Matushkin, N.Yu., Polyansky, O.P., Travin, A. V., 2009. Thermochronological models for the evolution of A-type leucogranites in the Neoproterozoic collisional orogen of the Yenisei Ridge. *Russ. Geol. Geophys.* 50 (5), 438–452.
- Vernikovskiy, V.A., Vernikovskaya, A.E., Kotov, A.B., Sal'nikova, E.B., Kovach, V.P., 2003. Neoproterozoic accretionary and collisional events on the western margin of the Siberian craton: new geological and geochronological evidence from the Yenisey Ridge. *Tectonophysics* 375, 147–168.
- Vernikovskiy, V.A., Vernikovskaya, A.E., Wingate, M.T.D., Popov, N.V., Kovach, V.P., 2007. The 880–864 Ma granites of the Yenisey Ridge, western Siberian margin: geochemistry, SHRIMP geochronology, and tectonic implications. *Precamb. Res.* 154, 175–191.
- Vernikovskiy, V.A., Vernikovskaya, A.E., Sal'nikova, E.B., Berezhnaya, N.G., Larionov, A.N., Kotov, A.B., Kovach, V.P., Vernikovskaya, I.V., Matushkin, N.Yu., Yasenev, A.

- M., 1998. Late Riphean alkaline magmatism in the western framework of the Siberian craton. *Dokl. Earth Sci.* 419, 226–230.
- Volobuev, M.I., Zykov, S.I., Stupnikova, N.I., 1976. Geochronology of Precambrian formations of the Sayan-Yenisey region of Siberia. In: *Actual Questions of Modern Geochronology*. Nauka Press, Moscow, pp. 96–123 (in Russian).
- Wan, Y., Liu, D., Xu, Z., Dong, C., Wang, Z., Zhou, H., Yang, Z., Liu, Z., Wu, J., 2008. Paleoproterozoic crustally derived carbonate-rich magmatic rocks from the Daqinshan area, North China Craton: geological, petrographical, geochronological and geochemical (Hf, Nd, O and C) evidence. *Am. J. Sci.* 308, 351–378.
- Whitney, D.L., Evans, B.W., 2010. Abbreviations for names of rock-forming minerals. *Am. Mineral.* 95, 185–187.
- Wiedenbeck, M., Alle, P., Corfu, F., Griffin, W.L., Meier, M., Oberli, F., Von Quadt, A., Roddick, J.C., Spiegel, W., 1995. Three natural zircon standards for U–Th–Pb, Lu–Hf, trace element and REE analysis. *Geostandard Newslett.* 19, 1–23.
- Williams, I.S., 1998. U–Th–Pb geochronology by ion microprobe. In: McKibben, M. A., Shanks, W.C., Ridley, W.I. (Eds.), *Applications of Microanalytical Techniques to Understanding Mineralizing Processes*. *Reviews in Economic Geology*, vol. 7, pp. 1–35.